

**Contract No:**

This document was prepared in conjunction with work accomplished under Contract No. DE-AC09-08SR22470 with the U.S. Department of Energy.

**Disclaimer:**

This work was prepared under an agreement with and funded by the U.S. Government. Neither the U. S. Government or its employees, nor any of its contractors, subcontractors or their employees, makes any express or implied: 1. warranty or assumes any legal liability for the accuracy, completeness, or for the use or results of such use of any information, product, or process disclosed; or 2. representation that such use or results of such use would not infringe privately owned rights; or 3. endorsement or recommendation of any specifically identified commercial product, process, or service. Any views and opinions of authors expressed in this work do not necessarily state or reflect those of the United States Government, or its contractors, or subcontractors.

# **A Case Study of Chlorine Transport and Fate Following a Large Accidental Release**

by

Robert L. Buckley<sup>a,\*</sup>

Charles H. Hunter<sup>a</sup>

David W. Werth<sup>a</sup>

Morgana T. Whiteside<sup>a</sup>

Kuo-Fu Chen<sup>a</sup>

- a. Savannah River National Laboratory, Savannah River Site, Aiken South Carolina 29808 United States. [robert.buckley@srnl.doe.gov](mailto:robert.buckley@srnl.doe.gov); [chuck.hunter@srnl.doe.gov](mailto:chuck.hunter@srnl.doe.gov); [david.werth@srnl.doe.gov](mailto:david.werth@srnl.doe.gov); [morgana.whiteside@srnl.doe.gov](mailto:morgana.whiteside@srnl.doe.gov); [kuo-fu.chen@srnl.doe.gov](mailto:kuo-fu.chen@srnl.doe.gov)

and

Carl A. Mazzola<sup>b</sup>

- b. Shaw Environmental, Inc., 4163 Hammond's Ferry Rd., Evans, Georgia 30809 United States. [carl.mazzola@shawgrp.com](mailto:carl.mazzola@shawgrp.com)

## **ABSTRACT**

A train derailment that occurred in Graniteville, South Carolina during the early morning hours of 06 January, 2005 resulted in the prompt release of approximately 60 tons of chlorine to the environment. Comprehensive modeling of the transport and fate of this release was performed including the characterization of the initial three-phased chlorine release, a detailed determination of the local atmospheric conditions acting to generate, disperse, and deplete the chlorine vapor cloud, the establishment of physical exchange mechanisms between the airborne vapor and local surface waters, and local aquatic dilution and mixing.

Previous studies of large chlorine releases have concluded that depletion of the resulting vapor cloud through physical and chemical reactions with sunlight, atmospheric constituents, and local surfaces can significantly reduce the areal extent over which the vapor poses a toxicological hazard. For Graniteville, modeling results were the most consistent with available data on human health effects, animal and fish mortality, and vegetation damage when an effective deposition velocity in the lower end of a range of values commonly cited in other studies ( $1 \text{ cm s}^{-1}$ ) was applied. This relatively small deposition is attributed to a lack of sunlight, a limited uptake in vegetation due to rapid stomatal damage, and the limited presence of nearby man-made structures. Explicit simulations of chlorine deposition into adjacent surface waters were based on a modified Henry's Law approach and resulted in the transfer of an estimated 21 kg of chlorine into these waters.

**Key Words:** atmospheric modeling; dispersion; chlorine release; deposition velocity; absorption

\*Corresponding author:

Dr. Robert L. Buckley

Savannah River National Laboratory

773A, A1008, Savannah River Site

Aiken, South Carolina 29808 United States

Phone: +1-803-725-1926; Fax: +1-803-725-4233

[robert.buckley@srnl.doe.gov](mailto:robert.buckley@srnl.doe.gov)

## 1. Introduction

The collision of two trains at a rail spur in the town of Graniteville, South Carolina in the early morning hours of 6 January, 2005 caused a catastrophic breach to a railcar containing chlorine. The sudden depressurization of the railcar's inner tank resulted in the rapid discharge of approximately two-thirds of the total contents (60 tons) of chlorine into the environment within a few minutes (NTSB, 2005). The discharged mixture of liquid and aerosols quickly vaporized and formed a dense cloud of chlorine vapor that settled toward the west and southwest into a shallow valley bisected by Horse Creek, which bounds Graniteville to the west. Over the next three hours, this dense chlorine cloud spread through gravitational settling, diffused into the ambient atmosphere, and was subsequently transported out of the area by the prevailing south-southwesterly wind. The resulting statistics on mortality, morbidity, and environmental damage included 9 fatalities and 71 hospitalizations, several hundred deaths of animal and fish, and a severe bleaching of vegetation within a radius of approximately 1 km of the accident scene (Allen and Thomason, 2005; Buckley et al, 2007; Wenck et al, 2007). A previous modeling study (Buckley et al., 2007) examined the release of chlorine from an emergency response perspective and provides further background information.

Graniteville is located in southwestern South Carolina in a region of gently sloping terrain. The derailment site lies in a shallow valley formed by Horse Creek which is oriented from north to south (Fig. 1). Land use in the area is generally suburban, with a textile mill and supporting facilities and parking lots adjacent to the derailment site. The prevailing south-southwesterly wind at the time of the collision was the result of clockwise circulation around a surface high pressure system centered off the southeast United States coast ahead of an advancing cold front (Fig. 2).

A modeling study was conducted to characterize in detail the transport and fate of this chlorine release through the air and surface waters in the immediate vicinity of Graniteville. All calculations for this study were based on a rapid discharge of 60 tons of the total inventory of 90 tons of product from the railcar (NTSB, 2005). Modeling studies of similar large chlorine releases, notably in Festus, Missouri and Macedonia, Texas, are summarized by Hanna et al. (2008a). To account for the effects of local topography, fine scale meteorological conditions were generated with the Regional Atmospheric Modeling System (RAMS, Pielke et al., 1992).

The SRNL has many years of experience with RAMS in both operational and research applications. Particular attention was placed on accurately characterizing the near-surface conditions that affected the initial generation of a large, dense cloud of chlorine vapor and the subsequent dispersion and depletion of this toxic cloud as it was transported over the study area. The calculations were run for three hours after the railcar was breached, a period that bounds the eventual dissipation of the release and subsequent transport out of the affected Graniteville area. The airborne transport and diffusion calculations were based on the Second-Order Closure Integrated Puff (SCIPUFF, Sykes et al., 1993, 1995) module of the Hazard Prediction Assessment Capability (HPAC, Sykes et al., 1998, 2004) code, using the detailed local meteorological conditions generated with RAMS. The HPAC-SCIPUFF suite was chosen for its proven ability to simulate dense gas releases, its effective widespread use by numerous other investigators, as well as its extensive benchmarking (e.g., Sykes et al., 1993; Cox et al., 1998, 2003; Chang et al., 2003; Hanna et al., 2007, 2008a, 2008b).

A unique aspect of the Graniteville release was the close proximity of navigable surface waters, including the Flat Rock and Bridge Creek ponds north of the derailment site, and Horse Creek. Absorption of the chlorine vapor by these waters, and the subsequent dilution and transport of the absorbed chlorine (as hydrochloric acid) were modeled with the Savannah River National Laboratory's ALGE model (Garrett et al., 2005; Blanton et al., 2009). Chlorine absorption rates were calculated using a Henry's Law approach modified for reactive chemicals.

In addition, published data on human health and environmental effects collected after the release provided considerable opportunity for evaluating model results, particularly with respect to important physical processes associated with reactive chemicals that are not explicitly simulated by current atmospheric dispersion models. For example, recent investigations have noted that the depletion of chlorine vapor through interactions with man-made structures can significantly reduce the distance over which the release poses an airborne human health hazard (Hanna and Chang, 2008; Dillon, 2009). The associated uncertainties are of significant concern to agencies responsible for transportation emergency planning (Goodwin and Donaho, 2010). For this study, a site specific characterization of chlorine vapor depletion was performed by evaluating a bounding range of values for the domain-averaged effective deposition velocity with respect to the available health and environmental effects data.

## 2. Environmental Modeling Techniques

### 2.1. Detailed Simulation of Local Meteorological Conditions

The RAMS model has been used successfully by numerous investigators to conduct refined, local scale simulations (e.g. Buckley and Kurzeja, 1997; Avissar et al., 1998; O'Steen and Werth, 2009), and has been determined to be useful for studying the relevant motions that characterize atmospheric flow phenomena at this particular scale.

The RAMS simulations of local meteorology in the Graniteville area were conducted using five nested grids with horizontal grid spacing of 20.48 km, 5.12 km, 1.28 km, 320 m, and 80 m (Fig. 3). The innermost grid covers an area about 7 km square, centered on a point north of the derailment site. The lateral boundary conditions were provided by output data from the National Centers for Environmental Prediction (NCEP) Rapid Update Cycle (RUC) model analysis (Benjamin et al., 2004), which is run at 3-hr intervals using an 81-km grid resolution. The vertical dimension uses a terrain-following coordinate system, which comprised 33 vertical levels for each grid, using a variable spacing that increased from 15 m at the lowest level to 1000 m at the highest level. A high resolution Light Detection and Ranging (LIDAR) topographic dataset with 10 m resolution (FEMA, 2003; USGS, 2006;) was used to more accurately resolve the microscale phenomena that result from the interactions between the local hills and valleys and the nighttime airflow (Fig. 1).

The Harrington radiative transfer scheme (Gabriel et al., 1998), which uses a two-stream approximation, was applied across all grids to both longwave and shortwave radiation. The Kuo cumulus scheme (Kuo, 1974), in which moisture convergence is converted to convective motion, was selected as the cumulus parameterization for the coarser grids (i.e., grids 1, 2 and 3), while a cloud prognostic scheme (Cotton et al., 1986; Meyers et al., 1992) was used for the two finer grids. The parameterization of the fluxes of heat and moisture from the ground surface was based on the Land Ecosystem-Atmosphere Feedback (LEAF-3) scheme (Walko et al., 2000). Each grid square (i.e., the area formed by four model grid points) is assigned a fraction of each of 21 land surface types, including water, and each type is assigned its own set of characteristic variables (e.g., leaf area index, albedo, etc.). The heat and moisture fluxes are calculated

individually for each surface type and then averaged to determine representative fluxes over a grid square.

Within the model atmosphere, unresolved mixing and turbulent transport of meteorological quantities by turbulent eddies is accommodated by the application of eddy diffusivity or  $K$ -theory. The method used to determine the magnitude of the eddy diffusivity is dependent on the eddy diffusion scheme. For all grids, the horizontal diffusivity is calculated as the product of the horizontal deformation and the length-scale squared (Smagorinsky, 1963). For vertical diffusivity, the Mellor-Yamada scheme (Mellor and Yamada, 1974) is invoked, by which a prognostic turbulence kinetic energy is calculated and used to determine the value of  $K$ . Determination of the lower (i.e. surface) boundary requires consideration of both ground conditions and surface characteristics. Ground conditions are characterized by the specification of initial soil temperature and soil moisture. Vegetation data, based on satellite observations from the Advanced Very High Resolution Radiometer (AVHRR) at 1 km resolution, are used in RAMS to assign values of albedo, surface vegetation roughness, thermal emissivity and other relevant model parameters.

The simulation for this study was initiated with a set of boundary conditions appropriate for 0000 UTC (1900 local time), 06 January, 2005 for grids 1, 2, and 3. The finer grids were inserted into the calculation six hours later (i.e., 0600 UTC) and detailed meteorological conditions were simulated until 1100 UTC. The meteorological data from the innermost (i.e., 5<sup>th</sup>) grid was then used as input for the transport and diffusion calculations using HPAC.

## *2.2 Source Term Characterization*

The collision produced an irregular tear in the inner insulated tank of the affected railcar approximately 0.8 m (30 in) in length and an average of 0.08 m (3 in) in width just above the mid-point of the tank (Fig. 4, photo courtesy of the South Carolina Department of Health and Environmental Control, SCDHEC, 2006). Chlorine is transported within the railcar as a pressurized cryogenic liquid. Exposure of the tank's contents to ambient atmospheric conditions resulted in a sudden depressurization of the chlorine, followed by a rapid vaporization (i.e., flashing) of the cryogenic liquid, and an energetic discharge of chlorine into the environment in the form of vapor, aerosols, and liquid.

A determination of the discharge rate and form of the initial release was performed with two codes: (1) the National Oceanic and Atmospheric Administration (NOAA) Areal Locations of Hazardous Atmospheres (ALOHA) code (Reynolds, 1992); and, (2) the Industrial Transportation (ITRANS) module of HPAC. Input data for the ALOHA calculations are summarized in Table 1. The railcar dimensions were taken from a specifications diagram contained in the HPAC data libraries for the railcar type identified by the NTSB (i.e., United States Department of Transportation type DOT-105J500W). Additional required input, such as the internal temperature of liquid in the tank, and the dimensions, orientation, and location of the rupture, were adopted from the NTSB report (NTSB, 2005). Photographs of the railcar taken by emergency response personnel at the scene, such as shown in Fig. 4, were used to verify additional ALOHA input requirements, such as the dimensions, location, and orientation of the breach on the railcar surface. For liquefied chemicals that exist as a gas at ambient temperatures and pressures, the discharge is simulated by ALOHA as a high-momentum, two-phase discharge of aerosol and gas (Reynolds, 1992). The aerosolized liquid is assumed by ALOHA to evaporate rapidly into a gas with no subsequent formation of a liquid puddle on the ground below the tank car.

The ALOHA calculation resulted in an estimated total chlorine release of 59,000 kg (65 tons) which is within 10% of the NTSB estimate. Due to the high storage pressure present within the tank, most of the discharge occurred in the first minute with a total release duration of 5 minutes. The likely occurrence of a short-duration release was corroborated by Hanna et al. (2008a) and Britter et al. (2009, 2010), in which detailed calculations of pressurized chlorine releases from irregular breaches of the size for the Graniteville accident were estimated.

Within HPAC, the ITRANS module does not allow an explicit specification of the damage incurred by the railcar, but it does provide useful output on all three thermodynamic forms of the source term that are likely to occur (i.e., aerosols, vapor, liquid pool). The ITRANS option resulting in the most realistically prompt evolution of the chlorine to a vapor cloud, as suggested by the ALOHA results and Britter et al. (2009), was selected for coupling with the subsequent simulations of atmospheric dispersion in SCIPUFF. This resulted in 26% (16 tons) of the discharge expelled in vapor form due to the immediate flashing from depressurization, 33% (20 tons) released in aerosol form, which is quickly evaporated as the aerosol droplets are exposed to the atmosphere, and the remaining 41% (24 tons) released as a liquid pool; all spread around the

derailment site. The release of vapor and aerosol was assumed to occur over a period of three (3) minutes, while the sub-cooled pooled liquid was assumed to be released instantaneously and then evaporated over time. All source term calculations conducted with the HPAC-ITRANS code were based on a source location at a height of 2 m above ground, with coordinates of 33.56219° N, -81.80856° E (NTSB, 2005).

### *2.3. Dense Gas Dispersion and Deposition*

Atmospheric transport, diffusion, and deposition were modeled using the SCIPUFF (Sykes et al., 1993, 1995) module within HPAC Version 5.0 (DTRA, 2008). SCIPUFF describes diffusion processes using second-order turbulence closure by relating the dispersion rate to turbulent fluctuations in wind direction and wind speed. The HPAC implementation of SCIPUFF contains a suite of programs to read in the gridded meteorological data generated by RAMS, interpolate it to a second user-defined grid defined within HPAC, and characterize in detail the thermodynamic evolution of the chlorine released from the railcar.

The range of time for the transport and dispersion calculations is three hours, from 0740 UTC (2:40 a.m. local time) to 1040 UTC (5:40 am local time), after which a substantial portion of the chlorine vapor from this initial large release had been either depleted through interaction with the terrestrial environment or transported out of the area. The RAMS-generated meteorological data, available at 2-minute intervals, were converted into the Multi-scale Environmental Dispersion over Complex Terrain (MEDOC) format for ingestion into HPAC. The MEDOC format requires data on a regularly-spaced latitude-longitude grid with vertical data on terrain-following height levels. Input data from RAMS included three-dimensional velocity components, potential temperature, vapor mixing ratio, topography, surface sensible heat flux, and planetary boundary layer height. The vertical grid for HPAC calculations consisted of 50 layers with spacing between 5 m and 10 m spanning the lowest 400 m of the atmosphere.

Output from RAMS was used to control most of the boundary layer calculations. Although terrain height was fed into SCIPUFF through RAMS input data, surface characteristics were not transferred. In this case, SCIPUFF required selection of a discrete surface cover category (e.g., desert, water, urban, grassland, cultivated, or forest). The area within a few hundred meter radius of the release consists mainly of paved parking lots and roads interspersed by open patches of grass, isolated trees, a few one- to two-story industrial structures and residential houses to the

east. Areas beyond the immediate vicinity of the derailment are primarily covered by mature pine trees.

An analysis of surface roughness length,  $z_0$ , using the EPA AERSURFACE program (EPA, 2008a) resulted in an estimated average roughness of about 0.7 meter for an area within a 1 km radius of the accident location. The AERSURFACE calculation is based on National Land Cover Data (NLCD) imagery for 1992 from the United States Geological Survey (USGS). This imagery defines 21 land surface categories at a 30-meter resolution. A  $z_0$  of 0.7 m is generally representative of a ground cover consisting of numerous medium to large obstacles such as hedges, trees, and small structures. Conversely, cultivated surfaces containing plantings of low to medium crops would be characterized by a roughness length less than 0.1 m (Stull, 1988).

Since little change in land use had occurred in the immediate area of Graniteville over the thirteen years prior to the accident, an estimated roughness length based on the 1992 imagery was considered reasonably representative of surface conditions at the time of the derailment. Therefore, 'forest' was selected in HPAC as the appropriate surface type.

As described previously, characterization of vapor cloud depletion is a critical component of this analysis. Generally, the chemical and/or physical responses of structural surfaces, pavement, soils, or vegetation following exposure to reactive gases such as chlorine are complex, highly variable in space and time, and poorly understood due to limited empirical data. Most models, particularly those that must execute quickly to support emergency response decision-making, simply ignore deposition/depletion of a chemical. As a result, these models significantly over-predict the true areal extent of the hazard (Hanna and Chang, 2008).

The amount of chlorine deposited on, or absorbed by, surfaces in contact with the airborne cloud can be parameterized through the specification of a surface-dependent dry deposition velocity,  $v_d$ . In general, actual values of  $v_d$  for a given chemical will be highly variable across the modeling domain due to: (1) the heterogeneous nature of the exposed surfaces (i.e., density and height of structures, variability in structural materials, and vegetation types), and (2) the diurnal and seasonal changes in plant physiology. Additional processes that can deplete chlorine vapor include chemical reactions with other atmospheric constituents, such as water vapor, and decomposition in sunlight through photolysis. Deposition models such as the resistance analog method have been developed to calculate  $v_d$  explicitly for some gases based on parameterizations of specific deposition processes; however, these models are still subject to considerable

uncertainty (Garrett and Murphy, 1981). Alternatively, SCIPUFF accepts the input of a single value for  $v_d$  that represents an aggregate deposition from all possible removal processes averaged over the entire modeling domain.

Suggested values of  $v_d$  for chlorine in the literature range from 0.5 cm s<sup>-1</sup> (EPA, 2005) to 2 cm s<sup>-1</sup> (Sehmel, 1984), to as high as 5 cm s<sup>-1</sup> (Hanna and Chang, 2008). For large releases, such as that occurring in Graniteville, Hanna and Chang (2008) have suggested that  $v_d$  may also vary as a function of the concentration of the depositing gas. Surfaces near the release that are exposed to extremely high concentrations could quickly become saturated with chlorine or undergo a chemical transformation which then limits additional deposition. Furthermore, Hill and Chamberlain (1974) describe experimental data that show the respiration of chlorine by vegetation becomes very small above an air concentration of 1 ppm due to damage to the plant's stoma. These phenomena, therefore, can lead to an abrupt and substantial reduction in the deposition velocity after only a small amount of time. Given such uncertainties, the calculations for this study are performed for three deposition cases: no deposition ( $v_d = 0$  cm s<sup>-1</sup>) and values of  $v_d$  equal to 1 cm s<sup>-1</sup> and 3 cm s<sup>-1</sup>.

#### *2.4. Aquatic Dilution and Mixing*

An estimate of aquatic absorption, dilution, and mixing of chlorine vapor deposited into the affected water bodies was performed with the SRNL ALGE model. ALGE is a three-dimensional hydrodynamic model used in comprehensive simulations of transport and diffusion of effluents (i.e., thermal, chemical, or radiological) discharged into water systems. ALGE includes a free-surface simulator, first-order chemical reactions, tracer transport, particle transport deposition/resuspension, and distribution coefficient-based modeling of chemical adsorption/desorption to particles. The model has been extensively used to simulate sediment and pollutant transport and thermal stratification in large lakes and estuaries (Garrett et al., 2005; Li et al., 2007; Blanton et al., 2009). ALGE is also used to compute transport, diffusion and deposition of aqueous tracers and has been validated against a unique radioactive tracer database (Blanton et al., 2009).

All calculations are performed on a three-dimensional computational domain describing the area and depth for each water body. The water bodies germane to this study are the blue shaded

areas in Fig. 5 and include Flat Rock Pond, Bridge Creek Pond, a canal flowing from Bridge Creek Pond (herein referred to as the unnamed canal), and Horse Creek, which flows from Flat Rock Pond. Details of the water bodies are presented in Table 2.

A rectangular domain for Flat Rock Pond, Bridge Creek Pond, and the canal was created, spanning roughly 1.5 km by 2.8 km in the east-west and north-south directions, respectively, with a grid spacing of roughly 10.3 m in length. Horse Creek was modeled separately for a region spanning 915 m by 2918 m, with a grid spacing slightly less than 4 m in length. There are three parameters associated with each grid element: whether a grid element covers a land surface or a water surface, the water body depth, and the concentration of the chemical within a thin film at the top of the water surface ( $C_{film}$ ).

### 2.5. Flow Determination

The flow velocity for ALGE was set equal to zero for Flat Rock Pond, the Bridge Creek Pond, and the canal, since onsite observations indicate a near-zero flow. The zero flow assumption potentially underestimates chlorine deposition, as it results in lower turbulent mixing within these water bodies. Hence, there is less transfer of chlorine across the air-water interface. In reality there is some small amount of turbulent mixing that would occur in these waters, which would add to the amount of chlorine absorbed from the air above.

The flows and gage heights of Horse Creek are monitored by the United States Geological Survey (USGS) at Gage Station-02196690 (referred to here as GS1 (USGS, 2009a)) located roughly 8 km southwest of the modeled portion of Horse Creek (Fig. 5) near its entrance into the Savannah River. The watershed of GS1 is approximately 400 square kilometers. However, there is no flow data available for 06 January, 2005 when the derailment took place. To compensate for this lack of data, a procedure was developed to estimate the flow at GS1 on the morning of 06 January, 2005 by correlating stream flow data with gage height data at GS1 for a 19-month period from 06 April, 2005 to 30 September, 2006. The Horse Creek flow rate at GS1 on 06 January, 2005 was estimated to be  $5.6 \text{ m}^3 \text{ s}^{-1}$  based on the observed gage height. The watershed area for the modeled section of the Horse Creek near Graniteville was determined to be  $163 \text{ km}^2$ . Assuming the flow rate is proportional to the watershed area, the flow in the modeled section of the Horse Creek near Graniteville on 06 January, 2005 was estimated to be  $2.0 \text{ m}^3 \text{ s}^{-1}$ .

## 2.6. Atmospheric and Aquatic Chemical Interactions

The airborne chlorine concentrations calculated by HPAC-SCIPUFF as a function of space and time are used as input to the ALGE model. It should be noted that the grid spatial structure used in the HPAC-SCIPUFF simulation differs from the grid structure used in ALGE. Therefore, a bilinear interpolation method was used to convert the chlorine concentrations generated by HPAC-SCIPUFF onto the grid structure used by the ALGE model. This interpolation will have little effect on the ALGE model results since the HPAC-SCIPUFF concentrations vary by only a small amount relative to the distance between grid points. Furthermore, only chlorine input from the initial release's gas cloud will be considered in this study.

The rate of chlorine absorption, or flux ( $N$ ), is estimated using the resistance to mass transfer, represented by an overall mass transfer coefficient ( $K_W$ ), and the chlorine concentration gradient, expressed as

$$N = K_W (C_{film} - C_W). \quad (1)$$

In Eq. (1),  $C_{film}$  is the concentration of aqueous chlorine at the air/water interface at equilibrium (mass/volume), and  $C_W$  is the concentration of chlorine in the water at a given time (mass/volume). Eq. (1) can be integrated over time to determine the total mass flux of chlorine into the water during passage of the airborne plume. In conjunction with the interface area between water and air, the depth of the water body, the time of the exposure, and the mass transfer coefficient, ALGE can also determine an instantaneous chlorine concentration in the water.

### 2.6.1. Estimating Chlorine Concentration at Equilibrium ( $C_{film}$ )

Values for  $C_{film}$  can be determined as a function of air concentration, absolute temperature, and Henry's constant ( $H$ ) (i.e., the ratio of a gaseous compound that will dissolve in solution as a result of its exerted partial pressure). When physical absorption determines the concentration of a gaseous compound in solution (i.e., when the vapor pressure ( $P_b$ ) of the compound drives the

molecule into solution), Henry's law can be used to calculate the equilibrium chlorine concentration, as given in Eq. (2),

$$C_{film} = EP_b / H. \quad (2)$$

$E$  represents the enhancement factor which may be used when calculating the absorption of reactive gases (Perry and Pigford, 1953; Brunson and Wellek, 1970; Alper 1973; Sada and Kumazawa, 1974; Merchuk, 1977). The high reactivity of gasses, such as chlorine, yields enhanced absorption due to an increased concentration gradient caused by the concentration of chlorine at the water surface continually diminishing due to reactions with the water according to Eq. (3) (Vivian and Whitney, 1947; Aietat and Roberts, 1986; Leaist, 1986; Kohl and Nielsen, 1997; and Islam et al., 2000),



Table 3 gives a comparison of reference data (Perry et al., 1963) for measured chlorine equilibrium concentrations at 10°C and varying partial pressures to chlorine concentrations predicted by Henry's Law (Eq. (2)). The final column of Table 3 shows a ratio of the measured solubility to the predicted solubility, with ratio values ranging from 8.8 at the lowest partial pressure of chlorine available from Perry et al. (1963) to 1.2 at the highest partial pressure of chlorine. The ratio between the measured and predicted concentrations, accounted for with an enhancement factor, decreases as the partial pressure of chlorine increases, reflecting the dominance of the concentration gradient (i.e., Henry's Law) and the decreasing importance of the reactions of chlorine with water.

The peak partial pressure of chlorine above the water surface predicted by HPAC-SCIPUFF for this evaluation was approximately 977 ppm. As there is no reference data available at this low partial pressure, an enhancement factor had to be assumed. An enhancement factor of 8.8 ( $E$  in Eq. (2)) was used to predict  $C_{film}$  as this ratio represents the lowest pressure for which there is reference data for comparison. In addition, an 8.8 ratio is a conservative estimate as the enhancement factor is expected to be higher as indicated by the trend of Table 3.

## 2.6.2. Estimating the Mass Transfer Coefficient ( $K_W$ )

$K_W$  for the liquid phase was determined by combining the individual phase mass transfer coefficients for water and air,  $k_W$  and  $k_A$ , respectively, with Henry's constant (i.e., dimensionless, air/water concentration) according to

$$\frac{1}{K_W} = \frac{1}{k_W} + \frac{1}{Hk_A}. \quad (4)$$

There are a number of empirical formulae that have been developed for calculating  $k_W$  and  $k_A$  (MacKay and Matsunaga, 1973; Southworth, 1979; MacKay and Yeun, 1983; Springer et al., 1984; Thibodeaux, 1996; Tata et al., 2003). While the majority of these methods were derived for volatile organic carbons, the volatility of chlorine gas makes the comparison appropriate. For  $k_W$ , the key variables of water current and stream depth were assumed to be  $0.25 \text{ m s}^{-1}$  and  $0.8 \text{ m}$ , respectively (Table 2). These assumptions were based on a survey station near Horse Creek, Gage Station-02196689 (USGS, 2009b) and field observations. For  $k_A$ , a wind speed at  $10 \text{ m}$  above the surface at the time of the accident was taken from the NTSB final accident report to be  $3.1 \text{ m s}^{-1}$ , and an assumed total pond surface area of  $334,000 \text{ m}^2$  was based on spatial analysis of surface maps of the Flat Rock and the Bridge Creek Pond complex (NTSB, 2005). A temperature of  $10^\circ\text{C}$  at the time of the accident was used throughout the chlorine absorption analysis based on a temperature of  $12.8^\circ\text{C}$ , also presented in the NTSB (2005) report. A working temperature of  $10^\circ\text{C}$  was used rather than  $12.8^\circ\text{C}$  because reference data (i.e., density, viscosity, diffusion) is not as readily available for  $12.8^\circ\text{C}$  and  $10^\circ\text{C}$  provides a more conservative estimate of mass flux than  $15^\circ\text{C}$  (i.e. the resulting concentration of chlorine in the water will not be over-estimated).

Table 4 summarizes the results of the different empirical equations, the assumptions required to reach these values, and an average predicted  $k_W$  and  $k_A$ . The relatively high value of  $k_A$  indicates that the system is liquid-phase limited, or that the chlorine gas diffuses into the surface of the water much faster than the chlorine at the surface diffuses into the bulk liquid. In liquid-phase limited systems, the  $K_W$  will be equal to the  $k_w$ . As the estimation methods of Mackay and Yeun (1983) and Springer et al. (1984) do not account for the motion of water bodies (i.e., stream depth and current) they are best suited to simulate the slow moving water bodies of the

ponds and canal. Southworth (1979) and Thibedeaux (1996) do incorporate the motions of water bodies, the turbulence of which results in a higher mass transfer coefficient, and are therefore best suited for the simulation of fast-moving water bodies, such as Horse Creek. In order to encompass the range of conditions, two  $K_W$  values ( $1.6 \text{ cm h}^{-1}$  and  $6.8 \text{ cm h}^{-1}$ ) were used in calculations of chlorine mass transfer. These two values of  $K_W$  are the respective averages of the two low  $K_w$  values produced by Mackay and Yeun (1983) and Springer et al. (1984) and the two high  $K_W$  values produced by Southworth (1979) and Thibedeaux (1996). The lower  $K_W$  value was used in calculations of slow-moving water bodies (i.e., ponds and canals) while the higher value was used for the fast-moving water body (i.e., Horse Creek).

### 3. Results

#### 3.1 Simulated Meteorological Conditions

At the time of the Graniteville derailment, a moderate surface pressure gradient over the region resulted in a pronounced south-southwesterly wind. Locally, the presence of this flow appears to have counteracted the development of topography-driven microscale flows in the immediate Graniteville and Horse Creek Valley area. Near the surface, as shown in Fig. 6, winds were simulated to be generally south-southwesterly to southwesterly at speeds ranging from  $2 \text{ m s}^{-1}$  to  $6 \text{ m s}^{-1}$  on well-exposed hill tops to  $1 \text{ m s}^{-1}$  or less in the Horse Creek Valley. Moreover, a few isolated areas of near-stagnant flow are present (e.g., just to the southwest of the derailment site), and some small-scale terrain-induced channeling is also evident. Simulated temperatures show that a strong temperature inversion was present in the area that extended from just above the surface upward to 200 m AGL, as indicated in Fig. 7. In Fig. 7a, the soundings at two distinct times are taken at the tall tower site in Beech Island, South Carolina (denoted as “TV” in Fig. 3a), south of the derailment site. The simulated soundings at the derailment site (see Fig. 7b) have approximately the same inversion height, but are more intense as evidenced by the minimum temperature at the surface being  $12 \text{ }^\circ\text{C}$  to  $13 \text{ }^\circ\text{C}$ , with maximum temperature at  $16 \text{ }^\circ\text{C}$  to  $17 \text{ }^\circ\text{C}$  aloft. Based on the local surface observations, weak mechanical turbulence is believed to have been present in a shallow slightly stable surface layer (i.e., equivalent to a Pasquill stability class E). This turbulence may have been sufficient to enable a transfer of southwesterly

momentum from the stronger inversion layer above, toward the ground. Observations at the tall tower (see open markers in Fig. 7) indicate the presence of this inversion. Fig. 8 shows the meridional component of the simulated wind in a cross-section oriented east/west through the derailment site. Weak southerly up-valley flow is occurring at the valley floor, with stronger southerly flow on either side of the valley. This component of the flow becomes more pronounced at higher levels.

Model results were compared to available observations in the vicinity of Graniteville to assess the performance of the RAMS simulations. The three nearest surface observation sites are the SRNL Central Climatology station (SRS) and the National Weather Service (NWS) Automated Surface Observation System (ASOS) stations at Bush Field (AGS) and Daniel Field (DNL), both located in Augusta, Georgia (see Fig. 3a). These locations provide a sample of values over different terrain. A time-series comparison of observed and simulated winds is shown in Figs. 9a and 9b. The relative magnitude of observed and simulated wind speed varies somewhat among the observing stations. The simulated wind speeds are stronger than the observed values at SRS, which is in a heavily forested location. Conversely, simulated wind speeds are generally weaker than the observed values at the two Augusta airport locations (AGS and DNL, Fig. 9a). The simulated values for wind speed at Graniteville lie in the mid-range between these three datasets. The observed wind direction is from the southwest to south-southwest over the Augusta area, and the modeled wind direction is in strong agreement as shown in Fig. 9b. Based on the comparison of these observations with the synoptic scale conditions and flow regimes for this type of terrain, it is judged that RAMS is producing a reasonable representation of local meteorological conditions that occurred on the night of the derailment.

## *3.2. Dense Gas Transport and Dispersion*

### *3.2.1. SCIPUFF Concentration Estimates*

The evolution of the chlorine plume over the 3-hr simulation period is illustrated by the contours of integrated surface dose in Fig. 10 and contours of instantaneous concentration in Fig. 11. In Fig. 10, plots of the maximum 1-hour integrated ground-level concentration representing

chlorine dose that occurred over the 3-hour period of simulation are shown for the no deposition case ( $v_d = 0$ ) and deposition cases with  $v_d$  equal to  $1 \text{ cm s}^{-1}$  and  $3 \text{ cm s}^{-1}$ .

It is clear from Fig. 10 that the higher values for deposition velocity lead to correspondingly smaller chlorine footprints. Furthermore, for the cases with  $v_d > 0$ , the yellow 20 ppm contour appears to reasonably approximate the visual evidence from the NTSB report which stated that the chlorine cloud spread out approximately 0.33 km (1000 ft) to the east and west, approximately 0.30 km (900 ft) to the south, and approximately 0.82 km (2500 ft) to the north shortly after the derailment (NTSB, 2005).

The SCIPUFF-simulated plume (Fig. 11) spreads generally with the terrain (i.e., oriented north-south) both initially, at the 10-minute time step, and at later times as shown for the 20- to 120-minute time steps. As expected with gravity-driven dense gas releases, higher concentrations and a greater vertical extent of the vapor cloud tended to occur in the lower-lying areas near Horse Creek where pine trees were bleached to the midpoint of their crowns (Buckley et al., 2007). In contrast, bleaching in the residential areas on higher terrain to the east was limited to just a few meters above ground. The general orientation of the plumes depicted in Fig. 11 and the dose footprints shown in Fig. 10 indicate an influence of both a gravity-driven flow of dense vapor toward the west and southwest initially, followed by a deformation of the plume towards the northeast through the Graniteville region under the effect of the prevailing south-southwesterly winds (Buckley et al., 2007). Later in the simulation, the concentrations decrease as the dense cloud spreads over a broader area. As the cloud progressively loses the characteristics of a dense gas through the entrainment of neutrally-buoyant ambient air, it begins to disperse passively and is transported toward the northeast.

### 3.2.2 Comparisons of SCIPUFF Results to Health and Environmental Effects Data

The chlorine footprints in Figs. 10 and 11 were subsequently compared to various toxicological benchmarks, available data on human health outcomes, reports of animal and fish mortality, and observations of vegetation damage (Buckley et al., 2007). Concentration thresholds equal to EPA's Acute Exposure Guideline Levels (AEGLs) (EPA, 2008b) for chlorine were used to evaluate modeled concentrations with respect to the reported health effects. The AEGL-2 and AEGL-3 level thresholds are 2 ppm and 20 ppm, respectively, for a 60-min

exposure (the green and yellow contours in Fig. 10) and 2.8 ppm and 50 ppm, respectively, for a 10-minute exposure. The AEGL-2 level represents the airborne concentration above which the general population, including susceptible individuals, could experience irreversible or other serious, long-lasting, adverse health effects or an impaired ability to escape. The AEGL-3 level represents the airborne concentration above which the general population, including susceptible individuals, could experience life-threatening health effects or death. Additional toxicological benchmarks associated with acute human exposure to chlorine include the occurrence of toxic pneumonitis and pulmonary edema for a one-hour exposure to concentrations of 40-60 ppm. Furthermore, death occurs for an exposure to concentrations of 430 ppm for 30 minutes or 1000 ppm for an exposure of a few minutes (IPCS, 1998). Moreover, a concentration of 5 ppm has been shown by studies to represent a bounding threshold for vegetation damage over an exposure of two hours (Sikora and Chappelka, 1996). Other studies have shown that exposure to chlorine concentrations as low as 0.1 – 5 ppm for two hours or more can damage pine trees.

Extensive epidemiological assessments of Graniteville residents affected by the chlorine release were conducted by several investigators (Wenck et al., 2007; Van Sickle et al., 2007; Van Sickle et al., 2009). Wenck et al. (2007) determined exposure morbidity outcomes based on interviews with several hundred people who sought medical care after the chlorine exposure. Affected individuals were assigned an exposure outcome rating ranging from 1 for no exposure to 5 for extreme exposure causing hospitalization for more than three nights, or death (Wenck et al., 2007). Therefore, an extreme outcome is generally consistent with the definition of the AEGL-3 threshold concentration.

Results from the SCIPUFF dispersion calculations for values of  $v_d$  ranging from 1.0 to 3.0  $\text{cm s}^{-1}$  were plotted along with the human exposure outcome data and observed vegetation damage. Model results were found to be the most consistent with the effects data for a  $v_d$  equal to 1.0  $\text{cm s}^{-1}$ . Results for this case are depicted in Figs. 10 and 11. Moderate to extreme exposures, represented by the yellow, orange and red dots in the two figures, are bounded appropriately by the AEGL-2 and AEGL-3 threshold levels, in virtually all of the reported cases. Locations of the nine fatalities were all within the 500 ppm contour shown in Fig. 11a where brief exposures to concentration approaching 1000 ppm could be reasonably expected. These results are also consistent with an assessment of animal mortality by SCDHEC (SCDHEC, 2006).

Model results for the no deposition case suggest concentrations capable of producing widespread vegetation damage extended much further to the north than was observed. In addition, virtually no adverse health effects were reported in residential areas to the north where model-estimated concentrations exceeded the AEGL-3 values. Conversely, modeling results for  $v_d$  equal to  $3.0 \text{ cm s}^{-1}$  show concentrations much too low to explain either observed vegetation damage or health effects data. A similar assessment for  $v_d$  equal to  $2.0 \text{ cm s}^{-1}$  (not shown) also appears to reduce concentrations too much to support the observed health effects data and vegetation damage.

Although some investigators have suggested deposition velocities for chlorine as high as  $5 \text{ cm s}^{-1}$ , several factors are believed to have limited depletion of the Graniteville plume. (1) The release occurred at night thereby eliminating the possibility of photolytic decomposition. (2) In addition to the time of day, the release occurred during the winter dormant period for vegetation which results in relatively low plant respiration rates. (3) Buildings in the area are generally low and scattered which also limits the total surface area available for interacting with the chlorine vapor, particularly in the vertical. Hanna and Chang (2008), for example, documented depletion rates up to  $5 \text{ cm s}^{-1}$  for a simulated chlorine release in an urban setting; however, this value was attributed to the interaction of the vapor with presence of ample vertical surface area. (4) Finally, the extremely high chlorine vapor concentration occurring soon after the release likely resulted in absorbing surfaces becoming saturated with chlorine, rapid depletion of reactive species on structural surfaces, or prompt damage to stoma of the exposed plants, preventing further respiratory uptake.

### *3.3. Aquatic Concentration*

Chlorine concentration estimates generated by HPAC-SCIPUFF for the  $1.0 \text{ cm s}^{-1}$  dry deposition velocity were input to the ALGE model to estimate total deposition of chlorine into Horse Creek, the unnamed canal, and the Flat Rock and Bridge Creek ponds over the period that chlorine from the initial large release was present in the Graniteville area. The calculation for Horse Creek was based on an average depth of  $0.8 \text{ m}$ , an estimated stream flow of  $2.0 \text{ m}^3 \text{ s}^{-1}$ , and an average mass transfer coefficient for moving water of  $6.8 \text{ cm hr}^{-1}$ , which resulted in an estimated total deposition of  $19 \text{ kg}$  of chlorine into Horse Creek. Similar calculations for the Flat

Rock and Bridge Creek ponds and the unnamed canal resulted in a total chlorine deposition of 1.1 kg and 0.55 kg, respectively. These calculations were based on the assumption that the water surface exhibited no discernible flow, and an average mass transfer coefficient for quiescent water of  $1.6 \text{ cm hr}^{-1}$ .

Model-estimated instantaneous concentrations of total chlorine for various locations along Horse Creek are shown in Fig. 12. These locations are represented by the diamonds in Fig. 5. The plots show that concentrations increased rapidly at locations to the west and southwest of the derailment site, as the core of the dense chlorine cloud settled into the shallow valley. Total chlorine concentrations in Horse Creek peaked as high as  $1.2 \text{ g m}^{-3}$  at location D from a combination of deposition directly from the atmosphere and the transport of chlorine from deposition occurring upstream (e.g., location C). Aqueous concentrations exceeded  $0.3 \text{ g m}^{-3}$  for nearly an hour at these locations after which the airborne cloud began to dissipate and chlorine in the water began to diffuse back into the relatively clean air above it.

Fig. 12b illustrates the estimated aqueous concentrations in both ponds and the canal. Instantaneous concentrations at selected locations, represented by the squares in Fig. 5, increased rapidly in the first thirty minutes as the cloud was transported northward. Instantaneous concentrations in Bridge Creek Pond reached a maximum of  $0.012 \text{ g m}^{-3}$  then slowly decreased as the airborne cloud dispersed and chlorine in the pond water began to diffuse back into the atmosphere. In the lower end of the canal (i.e., location A), the ALGE calculation yielded a much higher peak concentration of  $0.039 \text{ g m}^{-3}$  due to its close proximity to the derailment site. The instantaneous chlorine concentration in the canal quickly reached equilibrium with the air concentration after which no further transfer of chlorine into the canal occurred. An investigation of fish mortality in Horse Creek conducted by the South Carolina Department of Health and Environmental Control in the days after the derailment confirmed deaths of more than 100 bluegill and 34 yellow perch, as well as 16 other fish species in smaller numbers (Allen and Thomason, 2005). Published values of the  $LC_{50}$  (the lethal concentration for 50% of the exposed population) for these species suggest concentrations of chlorine in the creek that are consistent with the ALGE estimates. For example, Roseboom and Richey (1977) report  $LC_{50}$  values for bluegill approaching  $1 \text{ g m}^{-3}$  for an exposure time of a few hours. An  $LC_{50}$  of  $0.85 \text{ g m}^{-3}$  for a 65 minute exposure is reported by Cooke and Schreer (2010) for yellow perch. A more direct comparison of model results to the  $LC_{50}$  values could not be performed since the total population

of fish in the affected area of Horse Creek is not known. Concentrations predicted by ALGE for Bridge Creek and Flat Rock ponds were below the LC<sub>50</sub> levels for both species. No fish deaths from these ponds were reported.

#### **4. Potential Uncertainties**

Potential uncertainties in environmental transport models for toxic industrial chemicals (TIC) and their input parameters were assessed.

##### *4.1 Atmospheric Modeling Uncertainties*

Hanna and Chang (2008) identify several areas of weakness in modeling toxic industrial chemical (TIC) releases. The characterization of source term is affected by the complex thermodynamic behavior of TICs at the point of release, which is highly sensitive to the geometry of the puncture and prevailing environmental conditions. There is the very likely possibility of two-phase flow formation at three points: (1) within the tank; (2) at the hole in the tank; and, (3) just outside the hole in the tank, all of which affect the rate at which the gas plume evolves. Following the release, uncertainty exists in the initial spread of the resultant dense cloud and its subsequent depletion through interactions with the environment. If wind speeds are very light (i.e., approaching zero), then the effective evaporation release rate from the liquid pool is decreased, and downwind concentrations would be lower. The wind speed at which this phenomenon occurs is not precisely known. However, the wind speeds in Graniteville at the time of the derailment appear to have been sufficiently high that a slow evaporation scenario is less likely to have occurred.

Sensitivities of the model results to deposition velocity have previously been discussed. Although the comparison of modeling results to the available health and environmental effects data suggests an average deposition velocity of around 1 cm s<sup>-1</sup>, this value may have approached zero in the core of the highly concentrated dense cloud, possibly resulting in local underestimates of actual surface concentrations in some areas.

##### *4.2 Aquatic Modeling Uncertainties*

The principal uncertainties in aquatic dilution modeling include the depth of Horse Creek at the time of the derailment and the chlorine mass transfer coefficients ( $k_W$ ). The  $k_W$  values themselves are dependent on the assumed creek depth (0.8 m) (Table 2). A higher creek depth (e.g., 0.9 m) results in decreased  $k_W$ , while a lower creek depth (e.g., 0.5 m) results in increased  $k_W$ . As discussed, average values for  $k_W$  in Horse Creek were based on data shown in Table 4 (Southworth, 1979; Thibodeaux, 1996) for an assumed depth of 0.8 m. For the ponds and the water canal, the depth is assumed constant and the bounding  $k_W$  that can be used are given by MacKay and Yeun (1983) and Springer et al. (1984). The use of the average value from two methods of calculating  $k_W$  also introduces a degree of uncertainty. A sensitivity study conducted for possible variations in the values for the depth of Horse Creek and mass transfer coefficient calculation differences from Table 4 indicate variations in the total mass uptake of a factor of approximately two.

## 5. Conclusions

A detailed, multi-media modeling simulation was conducted of the initial discharge and subsequent transport and fate of approximately 60 tons of chlorine that was released into the environment following a train derailment that occurred in Graniteville, South Carolina during the early morning of 06 January, 2005. The modeling examined the formation of an initially dense chlorine vapor cloud, the dispersion of the vapor cloud within the Graniteville and Horse Creek valley area using detailed simulations of local meteorology, and the absorption and transport of chlorine in Horse Creek and nearby ponds. The results were evaluated with respect to observed vegetation damage, published data on human health effects, and fish mortality.

As noted by previous investigators (Hanna and Chang, 2008), deposition/depletion rates of reactive chemicals in the environment can vary significantly with respect to the time of day and characteristics of the surface with which the vapor cloud interacts. This has significant implications for hazard predictions that support decision makers in emergency planning and response. For the Graniteville release, modeling results were found to be reasonably consistent with the available environmental health effects and fish mortality data when the domain-averaged effective deposition velocity was set to  $1 \text{ cm s}^{-1}$ . Although some investigators have

suggested values for chlorine as high as  $5 \text{ cm s}^{-1}$ , several factors are believed to have limited depletion in this case of the Graniteville plume. The release occurred during a winter night which eliminated the possibility of photolytic decomposition and corresponds to a relative minimum in plant respiration. In addition, the nature of the surrounding surface, i.e., suburban with only low scattered structures, acted to minimize the total surface area that was available to potentially interact with the vapor cloud.

Using a modified Henry's Law approach, a total of 21 kg of chlorine was estimated to have deposited into the surface waters of interest. The estimate is believed to be lower than the actual deposition, as the enhancement factor that was applied to Henry's Law for reactive gases was assumed to be equal to that of the lowest partial pressure of chlorine for which there was experimental data. The empirical trend in this enhancement factor as a function of partial pressure of the gas suggests a greater flux of chlorine into the water would likely have occurred. Even so, predicted concentrations of chlorine in Horse Creek were reasonably consistent with published values of the  $LC_{50}$  for two species of fish that were observed to have had experienced significant deaths following the incident. A sensitivity analysis for the aqueous deposition calculations, based on potential uncertainty in stream depth for Horse Creek and the mass transfer coefficient suggested variations in the estimated total deposition of a factor of two. These comparisons corroborated the choices in model variables and confirmed the ability of the integrated modeling used in this study to estimate the actual physical processes that took place at the time of and subsequent to the derailment with reasonable reliability and certainty.

## References

Aietat, E.M., Roberts P.V., 1986. Application of mass-transfer theory to the kinetics of a fast gas-liquid reaction: Chlorine hydrolysis. *Environ. Sci. Technol.* 20, pp. 44-50.

Allen, D. E., C. S. Thomason, 2005. Fish Kill Investigation Graniteville Chlorine Spill Fish Kill Investigation in the Horse Creek System in Aiken County, SC January 7, 2005 through January 24, 2005. Division of Wildlife and Freshwater Fisheries, South Carolina Department of Natural Resources, EPA-005706).

Alper, E., 1973. Gas absorption with second-order reaction-comparison of approximate enhancement factor equations. *Chemical Engineering Science* 28 (11), pp. 2092-2093.

Avissar, R., Eloranta, E.W., Gürer, K., Tripoli, G. J., 1998. An Evaluation of the Large-Eddy Simulation Option of the Regional Atmospheric Modeling System in Simulating a Convective Boundary Layer: A FIFE Case Study. *Journal of Atmospheric Sciences* 55, 1109–1130.

Benjamin, S. G., Grell, G., Brown, J. M., Smirnova, T. G., Bleck R., 2004. Mesoscale weather prediction with the RUC hybrid isentropic — terrain-following coordinate model; *Monthly Weather Review* 132, pp. 473-494.

Blanton, J. O., Garrett, A. J., Bollinger, J. S., Hayes, D. W., Koffman, L. D., Amft, J., 2009. Transport and dispersion of a conservative tracer in coastal waters with large intertidal areas. *Estuaries and Coasts* 32 (3), pp. 573-592.

Britter, R., Weil, J., Leung, J., Hanna, S., March 31, 2009. Worked Examples using Improved Source Emission Models, Draft Task 5 Report under the Project: Toxic Industrial Chemical (TIC) Source Emissions Model Improvements. Hanna Consultants. Prepared for Defense Threat Reduction Agency, Contract Number HDTRA1-07-C-0082, Report Number P098-5.

Britter, R., Weil, J., Leung, J., Hanna, S., 2010. Toxic industrial chemical (TIC) source emissions modeling for pressurized liquefied gases. *Atmospheric Environment* 45, 1-25.

Brunson, R.J., Wellek, R.M., 1970. Determination of enhancement factor for mass transfer with an instantaneously fast chemical reaction. *Chemical Engineering Science* 25 (5), pp. 904.

Buckley, R.L., Kurzeja, R. J., 1997. An Observational and Numerical Study of the Nocturnal Sea Breeze. Part I: Structure and Circulation. *Journal of Applied Meteorology* 36, 1577–1598.

Buckley, R. L., Hunter, C. H., Addis, R. P., Parker, M. J., 2007. Modeling dispersion from toxic gas released after a train collision in Graniteville, SC. *Journal of the Air and Waste Management Association* 57, 268-278.

Chang, J. C., Franzese, P., Chayantrakom, K., Hanna, S. R., 2003. Evaluations of CALPUFF, HPAC, and VLSTRACK with two mesoscale field datasets. *Journal of Applied Meteorology* 42, 453-466.

Cooke, S. J., Schreer, J. F., 2010. Additive Effects of Chlorinated Biocides and Water Temperature on Fish in Thermal Effluents with Emphasis on the Great Lakes, *Reviews in Fisheries Science*, Vol 9, 69-113.

Cotton, W. R., G. J. Tripoli, R. M Rauber, and E. A. Mulvihill, 1986. Numerical simulation of the effects of varying ice crystal nucleation rates and aggregation processes on orographic snowfall. *Journal of Climate and Applied. Meteorology* 25, 1658-1680.

Cox, R. M., Sontowski, J., Fry Jr., R. N., Dougherty, C. M., Smith, T. J., 1998. Wind and diffusion modeling for complex terrain. *Journal of Applied Meteorology* 37 (10), 996-1009.

Cox, R. M., Sontowski, J., Dougherty, C. M., Boutet, C. J., 2003. The use of diagnostic and prognostic windfields for atmospheric transport calculations: an evaluation of the DIPOLE EAST 169 field experiment. *Meteorological Applications* 10, 151-164.

Defense Threat Reduction Agency (DTRA), January 2008. Hazard Prediction and Assessment Capability, On-Line Help, Version 5.0. For further information contact DTRA, Operational Applications Division Consequence Branch (TDOC) at (703) 767-3419.

Dillon, E. B., 2009. The Role of Deposition in Limiting the Hazard Extent of Dense-gas Plumes. *Journal of Hazardous Materials* 164, 1293-1303.

Environmental Protection Agency (EPA), 2005. Human Health Risk Assessment Protocol for Hazardous Waste Combustion Facilities. Office of Solid Waste and Emergency Response, United States Environmental Protection Agency, EPA530-R-05-006, Chapter 3.

Environmental Protection Agency (EPA), 2008a. AERSURFACE User's Guide, U. S. EPA Office of Air Quality Planning and Standards, EPA-454/B-08-001.

Environmental Protection Agency (EPA), 2008b. Acute Exposure Guideline Levels, <http://www.epa.gov/oppt/aegl/pubs/chemlist.htm> (accessed 10 July 2012).

Federal Emergency Management Agency (FEMA), 2003. Guidelines and Specifications for Flood Mapping Partners. Appendix A: Guidance for Aerial Mapping and Surveying, [http://www.fema.gov/plan/prevent/fhm/dl\\_cgs.shtm](http://www.fema.gov/plan/prevent/fhm/dl_cgs.shtm), (accessed 10 July 2012).

Gabriel, P., J. Harrington, G. Stephens, and T. Schneider, 1998. Adjoint Perturbation Method Applied to Two-Stream Radiative Transfer. *Journal of Quantitative Spectroscopy and Radiative Transfer* 59 (112), 1-24.

Garrett, A. J., Murphy, Jr., C. E., 1981. A PUFF-PLUME Atmospheric Deposition Model for Use at SRP in Emergency Response Situations. DP-1595.

Garrett, A. J., Bollinger, J. S., Hayes, D. W., 2005. Analysis of tritium transport in flooded South Carolina Savannah River floodplain, ANS 2005 Winter Meeting, Washington, DC, November 13 – 17.

Goodwin, Jr., B. S., Donaho, J. C., 2010. Tropical storm and hurricane recovery and preparedness strategies. *Institute for Laboratory Animal Research Journal* 51, 104-119.

Hanna, S. R., Chang, J. C., White, J. M., Bowers, J. F., 2007. Evaluation of the HPAC Dispersion Model with the Joint Urban 2003 (JU2003) Tracer Observations, Urban Environment. 7<sup>th</sup> Symposium on the Urban Environment (Paper 10.1), American Meteorological Society, 10-13 September 2007, San Diego, California (United States). AMS Headquarters, 45 Beacon Street, Boston, MA 02108-3693 (United States).

Hanna, S., Dharmavaram, J., Zhang, J., Sykes, I., Witlox, H., Khajehnajafi, S., Koslan, K., 2008a. Comparison of Six Widely-Used Dense Gas Dispersion Models for Three Recent Chlorine Railcar Accidents. *Process Safety Progress* 27 (3), 248-259.

Hanna, S., Hendrick, E., Santos, L., Reen, B., Stauffer, D., Deng, A. J., McQueen, J., Tsidulko, M., Janjic, Z., Sykes, R. I. 2008b. Comparison of Observed, MM5 and WRF-NMM Model-Simulated, and HPAC-Assumed Boundary-Layer Meteorological Variables for Three Days During the IHOP Field Experiment. 15<sup>th</sup> Joint Conference on Applications of Air Pollution Meteorology with the A&WMA (Paper 1.2), American Meteorological Society 88<sup>th</sup> Annual Meeting, 20-24 January 2008, New Orleans, Louisiana (United States). AMS Headquarters, 45 Beacon Street, Boston, MA 02108-3693 (United States).

Hanna, S., Chang, J., 2008. Gaps in toxic industrial chemical (TIC) model systems. *Croatian Meteorological Journal* 43 (43), 13-18.

Hill, A. C., Chamberlain, Jr., E. M., 1974. The removal of water soluble gases from the atmosphere by vegetation. ERDA Symposium Series 38, Atmosphere-Surface Exchange of Particulate and Gaseous Pollutants. Coordinators: R. J. Engelmann, U.S. Atomic Energy Commission and G. A. Sehmel, Battelle, PNNL.

International Program of Chemical Safety (IPCS), 1998. IPCS INCHEM Database for Chlorine, Poisons Information Monographs (PIM) 947. Available online at [www.inchem.org/documents/pims/chemical/pim947.htm](http://www.inchem.org/documents/pims/chemical/pim947.htm) (accessed 10 July 2012).

Islam, M. R., Kalam, M. R., Khan, M. R., 2000. Reactive gas solubility in water: an empirical relation. *Ind Eng. Chem. Res.* 39, pp. 2727-2630.

Kohl A.L., Nielsen, R. B., 1997. *Gas Purification*, Gulf Professional Publishing.

Kuo, H., 1974. Further studies of the parameterization of the influence of cumulus convection on large-scale flow. *Journal of Atmospheric Sciences* 31, 1232-1240.

Leaist, D.G., 1986. Absorption of chlorine into water. *Journal of Solution Chemistry* 15 (10), pp. 827-838.

Li, Y., Vodacek, A., Raqueno, N., Kremens, R., Garrett, A. J., Bosch, I., Makarewicz, J.C., Lewis, T.W., 2007. Circulation and stream plume modeling in Conesus Lake. *Environmental Modeling and Assessment*, doi: 10.1007/s10666-007-9090 x.

MacKay, D., Matsunaga, R., 1973. Evaporation rates of liquid hydrocarbon spills on land and water. *J. Chem. Eng.* 51, pp. 434-439.

MacKay, D., Yeun, A., 1983. Mass transfer coefficient correlations for volatilization of organic solutes from water. *Enviro. Sci. Tech.* 17, pp. 211-217.

Mellor G. L, Yamada, T., 1974. A hierarchy of closure models for planetary boundary layers, *Journal of Atmospheric Sciences* 31, 1791-1806.

Merchuk, J.C., 1977. Further considerations on enhancement factor for oxygen absorption into fermentation broth. *Biotechnology And Bioengineering* 19(12), pp. 1885-1889.

Meyers, M. P., DeMott, P. J., Cotton, W. R., 1992. New primary ice nucleation parameterizations in an explicit cloud model. *Journal of Applied Meteorology* 31, 708-721.

National Transportation Safety Board (NTSB), 2005. Collision of Norfolk southern freight train 192 with standing Norfolk southern local train P22 with subsequent hazardous materials released at Graniteville, South Carolina, January 6, 2005. Railroad Accident Report, ID: NTSB/RAR-05/04, PB2005-916304, Notation 7710A, Adopted November 29, 2005.

O'Steen, B. L., Werth, D. W. 2009. The Application of an Evolutionary Algorithm to the Optimization of a Mesoscale Meteorological Model. *Journal of Applied Meteorology and Climatology* 48 (2), 317-329.

Perry, R.H., Perry, J.H., Chilton, C.H., Kirkpatrick, S.D., 1963. *Chemical Engineers' Handbook*, McGraw-Hill.

Perry, R.H., Pigford, R.L., 1953. Kinetics of gas-liquid reactions - simultaneous absorption and chemical reaction. *Industrial and Engineering Chemistry* 45 (6), pp. 1247-1253.

Pielke R. A., Cotton, W. R., Walko, R. L., Tremback, C. J., Lyons, W. A., Grasso, L. D., Nicholls, M. E., Moran, M. D., Wesley, D. A., Lee, T. J., Copeland, J. H., 1992. A comprehensive meteorological modeling system--RAMS. *Meteorology and Atmospheric Physics* 49, 69-91.

Reynolds, M. R., 1992. ALOHA (Areal Locations of Hazardous Atmospheres) 5.0 Theoretical Description. NOAA Technical Memorandum NOS ORCA-65, Seattle, Washington (United States).

Roseboom, D. P., Richey, D. L., 1977. Acute Toxicity of Residual Chlorine and Ammonia to Some Native Illinois Fishes. ISWS/RI-85/77, Illinois State Water Survey, Urbana, IL.

Sada, E., Kumazawa, H., 1974. Variation of enhancement factor in gas absorption with order of chemical-reaction. *Chemical Engineering Science* 29 (2), pp. 335-338.

Sander, R., 1999. Compilation of Henry's law constants for inorganic and organic species of potential importance in environmental chemistry. Available online at <http://www.ceset.unicamp.br/~mariaacm/ST405/Lei%2520de%2520Henry.pdf> (accessed 10 July 2012).

Sehmel, G. A., 1984. Deposition and Resuspension. In: Randerson, D., ed. Chapter 12 in *Atmospheric Science and Power Production*, DOE/TIC-27601, 533-583.

Sikora, E. J., Chappelka, A. H., 1996. *Air Pollution Damage to Plants*, ACES Publications, ANR-0913: Alabama Cooperative Extension System, 1996. Available online at <http://www.aces.edu/pubs/docs/A/ANR-0913/ANR-0913.pdf> (accessed 10 July 2012).

Smagorinsky, J., 1963. General circulation experiments with the primitive equations. Part I, The basic experiment. *Monthly Weather Review* 91, 99-164.

South Carolina Department of Health and Environmental Control (SCDHEC), 2006. Graniteville, SC Train Derailment and Chlorine Release: Lessons Learned, Michael Spradlin. Available online at [http://www.astswmo.org/Files/Meetings/2006/2006-Hazardous\\_Waste\\_Conference/Chlorine-Gas-Train-Derailment-and-Cleanup.pdf](http://www.astswmo.org/Files/Meetings/2006/2006-Hazardous_Waste_Conference/Chlorine-Gas-Train-Derailment-and-Cleanup.pdf) (accessed 10 July 2012).

Southworth, G.R., 1979. The role of volatilization in removing polycyclic aromatic hydrocarbons from aquatic environments. *Bull. Environ. Contam. Toxicol.* 21, pp. 507-14.

Springer C., Lunney, P.D., Valsaraj, K.T., 1984. Emission of hazardous chemicals from surface and near surface impoundments to air. USEPA Solid and Hazardous Waste Research Division, Proj. Num. 808161-02.

Stull, R. B, 1988. *An Introduction to Boundary Layer Meteorology*, Kluwar Academic Publishers, Dordrecht, The Netherlands.

Sykes, R.I., Parker, S. F., and Henn, D.S., 1993. Numerical simulation of ANATEX tracer data using a turbulence closure model for long-range dispersion. *Journal of Applied Meteorology* 32, 929 – 947.

Sykes, R.I., Henn, D. S., 1995. Representation of velocity gradient effects in a gaussian puff model. *Journal of Applied Meteorology* 34, 2715 – 2723.

Sykes, R. I., Parker, S. F., Henn, D. S., Cerasoli, C. P., Santos, L. P., 1998. PC-SCIPUFF Version 1.2PD Technical Documentation. Titan Corporation, P. O. Box 2229, Princeton, New Jersey (United States).

Sykes, R. I., Parker, S. F., Henn, D. S., 2004. SCIPUFF Version 2.1 Technical Documentation. Titan Corporation, P. O. Box 2229, Princeton, New Jersey (United States).

Tata P., Witherspoon, J., Lue-Hing, C., 2003. *VOC Emissions from Wastewater Treatment Plants: Characterization, Control, and Compliance*. CRC.

Thibodeaux, 1996. *Environmental chemodynamics, Movement of chemicals in air, water, and soil*, John Wiley and Sons, New York.

United States Geological Survey (USGS, 2006): Light Detection and Ranging (LIDAR) Viewer. Available online at [http://lidar.cr.usgs.gov/LIDAR\\_View/](http://lidar.cr.usgs.gov/LIDAR_View/) (accessed 10 July 2012).

United States Geological Survey (USGS, 2009a): Available online at [http://waterdata.usgs.gov/nwis/dv/?site\\_no=02196690&agency\\_cd=USGS&referred\\_module=sw](http://waterdata.usgs.gov/nwis/dv/?site_no=02196690&agency_cd=USGS&referred_module=sw) (accessed 10 July 2012).

United States Geological Survey (USGS, 2009b): Available online at [http://waterdata.usgs.gov/nwis/dv/?site\\_no=02196689&agency\\_cd=USGS&referred\\_module=sw](http://waterdata.usgs.gov/nwis/dv/?site_no=02196689&agency_cd=USGS&referred_module=sw) (accessed 10 July 2012).

Van Sickle, D., Wenck, M. A., Belflower, A., Drocuick, D., Ferdinands, J., 2007. Panel Classification of Self-Reported Exposure Histories: A Useful Exposure Index After a Mass-Casualty Event, Public Health Reports, 122.

Van Sickle, D., Wenck, M. A., Belflower, A., Drocuick, D., Ferdinands, J., Holguin, F., Svendsen, E., Bretous, L., Jankelevich, S., Gibson, J. J., Garbe, P., Moolenaar, R. L., 2009. Acute Health Effects After Exposure to Chlorine Gas After a Train Derailment, The American Journal of Emergency Medicine, 27.

Vivian J.E., Whitney, R.P., 1947. Absorption of chlorine in water. Chemical Engineering Progress 43 (12), pp. 691-702.

Walko, R.L., Band, L.E., Baron, J., Kittel, T.G.F., Lammers, R., Lee, T.J., Ojima, D., Pielke, R.A., Taylor, C., Tague, C., Tremback, C.J., Vidale, P.L., 2000. Coupled Atmosphere–Biophysics–Hydrology Models for Environmental Modeling. Journal of Applied Meteorology 39, 931–944.

Wenck, M. A., Van Sickle, D., Drocuick, D., Belflower, A., Youngblood, C., Whisnant, M. D., Taylor, R., Rudnick, V., Gibson, J. J., 2007. Rapid Assessment of Exposure to Chlorine Released from a Train Derailment and Resulting Impact to Health. Public Health Reports 122.

**Table 1**

Input data for the ALOHA source release calculations

<b>Input Variable</b>	<b>Unit</b>	<b>Value</b>
Inside tank diameter	m	2.35
Inside tank length	m	12.8
Chemical mass in tank	tons	90
Percent full	dimensionless	100
Internal temperature	°C	-3.3
Average width of rupture	m	0.08
Length of rupture	m	0.8
Location of opening (from bottom of tank)	m	1.1

**Table 2**

Description of water bodies under study

<b>Parameter</b>	<b>Flat Rock Pond</b>	<b>Bridge Creek Pond</b>	<b>Unnamed Canal</b>	<b>Horse Creek</b>
Length	1000 m	800 m	1 km	3.8 km
Width	200 m	200 m	14 m	10 m
Depth	1.8 m*	2.5 m*	2 m**	0.8 m***
Orientation	North to South	West to East	North to South	North to South
Location <sup>†</sup>	2.5 km north	1.7 km north	500 m north	200 m west

\* Average representative depth based on sonar and manual depth measurements.

\*\* Average of two locations (ranging from 1.0 m to 2.2 m).

\*\*\* Average of four locations (ranging from 0.5 m to 0.9 m).

<sup>†</sup>Distance relative to the derailment site.

**Table 3**Ratio of actual solubility to that predicted by Henry's Law<sup>†</sup>

Partial Pressure, $P_{Cl}$ (ppm)	Reference Data	Solubility Predicted	<i>Actual Solubility/ Predicted Solubility</i>
	Solubility** (M)	by Henry's Law <sup>†</sup> ( $P_{Cl}/H$ ) (M)	
	<i>Actual Solubility</i>	<i>Predicted Solubility</i>	
$9.77 \times 10^2$	NA*	0.0001	NA*
$6.58 \times 10^3$	0.00635	0.0007	8.8
$1.32 \times 10^4$	0.008	0.0014	5.9
$3.95 \times 10^4$	0.014	0.0043	3.3
$6.58 \times 10^4$	0.019	0.0072	2.6
$1.32 \times 10^5$	0.029	0.0145	2.0
$1.97 \times 10^5$	0.038	0.0217	1.8
$2.63 \times 10^5$	0.047	0.0289	1.6
$3.29 \times 10^5$	0.056	0.0362	1.5
$3.95 \times 10^5$	0.064	0.0434	1.5
$4.61 \times 10^5$	0.072	0.0507	1.4
$5.26 \times 10^5$	0.080	0.0579	1.4
$5.92 \times 10^5$	0.088	0.0651	1.4
$6.58 \times 10^5$	0.096	0.0724	1.3
$7.24 \times 10^5$	0.104	0.0796	1.3
$7.89 \times 10^5$	0.112	0.0868	1.3
$8.55 \times 10^5$	0.120	0.0941	1.3
$9.21 \times 10^5$	0.128	0.1013	1.3
$9.87 \times 10^5$	0.136	0.1086	1.3
$1.05 \times 10^6$	0.144	0.1158	1.2

\* Reference data is unavailable at this pressure.

\*\* Taken from Perry et al., 1963.

<sup>†</sup> $H = 0.11 \times 10^6 \text{ M ppm}^{-1}$  (0.11 M atm<sup>-1</sup>), taken from Sander, 1999.

**Table 4**

Summary of transfer coefficient estimates

<b>Method</b>	<b><math>k_W</math> (cm h<sup>-1</sup>)</b>	<b><math>k_A</math> (cm h<sup>-1</sup>)</b>	<b>Assumptions</b>
MacKay and Matsunaga, 1973	NA	392	Wind speed and pond area
Southworth, 1979	4.8	1832	Stream depth and current
MacKay and Yeun, 1983	1.5	624	Wind speed
Springer et al., 1984	1.7	NA	Wind speed
Thibodeaux, 1996	8.7	NA	Stream depth and current

## List of Figures

Figure 1: Terrain in the area with contour intervals of 10 meters. Gray and purple shading denotes the lowest elevations, while red and pink shading indicates the highest elevations. Light gray shading indicates topographic elevation exceeding 50 m but less than 60 m AGL while light pink shading indicates topographic elevation exceeding 160 m AGL. The large black circle denotes the derailment site, while lighter lines indicate local roads.

Figure 2: Synoptic conditions at 1200 UTC (7:00 a.m. local time) January 6, 2005. (This figure is reproduced from Figure 5 of Buckley et al., 2007).

Figure 3: RAMS domains for (a) Outer grids 1, 2, and 3; and (b) Inner grids 4 and 5. The location of nearby meteorological observation towers are indicated with the diamonds labeled “SRS”, “TV”, “AGS”, and “DNL”.

Figure 4: Photograph of the tear in the tank car wall following the train derailment (photo courtesy of SCDHEC (2006)).

Figure 5: Map of water bodies considered in this study. The derailment site is indicated by the large red circle, while locations used to determine chlorine concentration are indicated by the diamonds (Horse Creek) and squares (lakes and canal). Letter designations are highlighted in Fig. 12.

Figure 6: Near surface wind vectors ( $\text{m s}^{-1}$ ) at 0740 UTC, 06 January, 2005. The black circle denotes the derailment site and contour lines indicate topography at 20 m intervals.

Figure 7: Comparison of simulated soundings for 0740 UTC (thick line) and 0900 UTC (thin line) on 06 January, 2005 at (a) the tall tower site (TV) in Beech Island, South Carolina and (b) the derailment site, with observed data at the climatology site at SRS (filled circle/square at the surface) and at the tall tower (open circle/square at 61 and 300 m). The square markers denote observations at 0740 UTC, while the circles are at 0900 UTC. Locations are noted in Fig. 3a.

Figure 8: (a) Meridional velocity (i.e., component of the wind blowing due north in  $\text{m s}^{-1}$ ) along an east-west cross-section through the derailment site at 0900 UTC (4:00 a.m. local time), January 6, 2005, at 84 m (crosses), 47 m (open circles), and 15 m (filled circles) above ground level. Axis labeling indicates distance in kilometers, and the arrow denotes the approximate location of the derailment. (b) Topographic height (m) along the same cross-section.

Figure 9: Comparison of simulated and observed (a) wind speed and (b) wind direction between 0700 and 1100 UTC, 06 January, 2005. Model data are interpolated to tower sites on RAMS Grid 2. Locations are noted as “SRS”, “DNL”, and “AGS” in Figure 3a.

Figure 10: Plots of integrated dose (60-min) for various dry deposition velocities ( $v_d$ ). The dose values (ppm of chlorine) are indicated in the legend. The bold purple line indicates approximate

vegetation damage, while the markers denote health effects as discussed in Section 3.2.2. The severity of the cases are ranked by color, where red is the most severe, followed by orange, yellow, green and blue, with blue being the least severe. (a)  $v_d = 0 \text{ cm s}^{-1}$ , (b)  $v_d = 1 \text{ cm s}^{-1}$ , and (c)  $v_d = 3 \text{ cm s}^{-1}$ .

Figure 11: Instantaneous concentration for  $v_d = 1.0 \text{ cm s}^{-1}$  at (a) 10 min, (b) 20 min, (c) 60 min, and (d) 120 min after the start of the release. The ground-level concentration values (ppm of chlorine) are indicated in the legend. The location of the derailment is indicated by the black circle. Markers denote health effects as in Figure 10.

Figure 12: Calculated chlorine concentrations ( $\text{g m}^{-3}$ ) as a function of time at selected location in (a) Horse Creek, and (b) the stagnant water bodies. The locations A to E are indicated in Fig. 5. The unlabeled lines represent much lower concentrations at other marked locations (indicated in Fig. 5 as diamonds along Horse Creek, and squares within the other water bodies).

*NOTE: Color figures are Figures 1, 4, 5, 6, 10 and 11.*

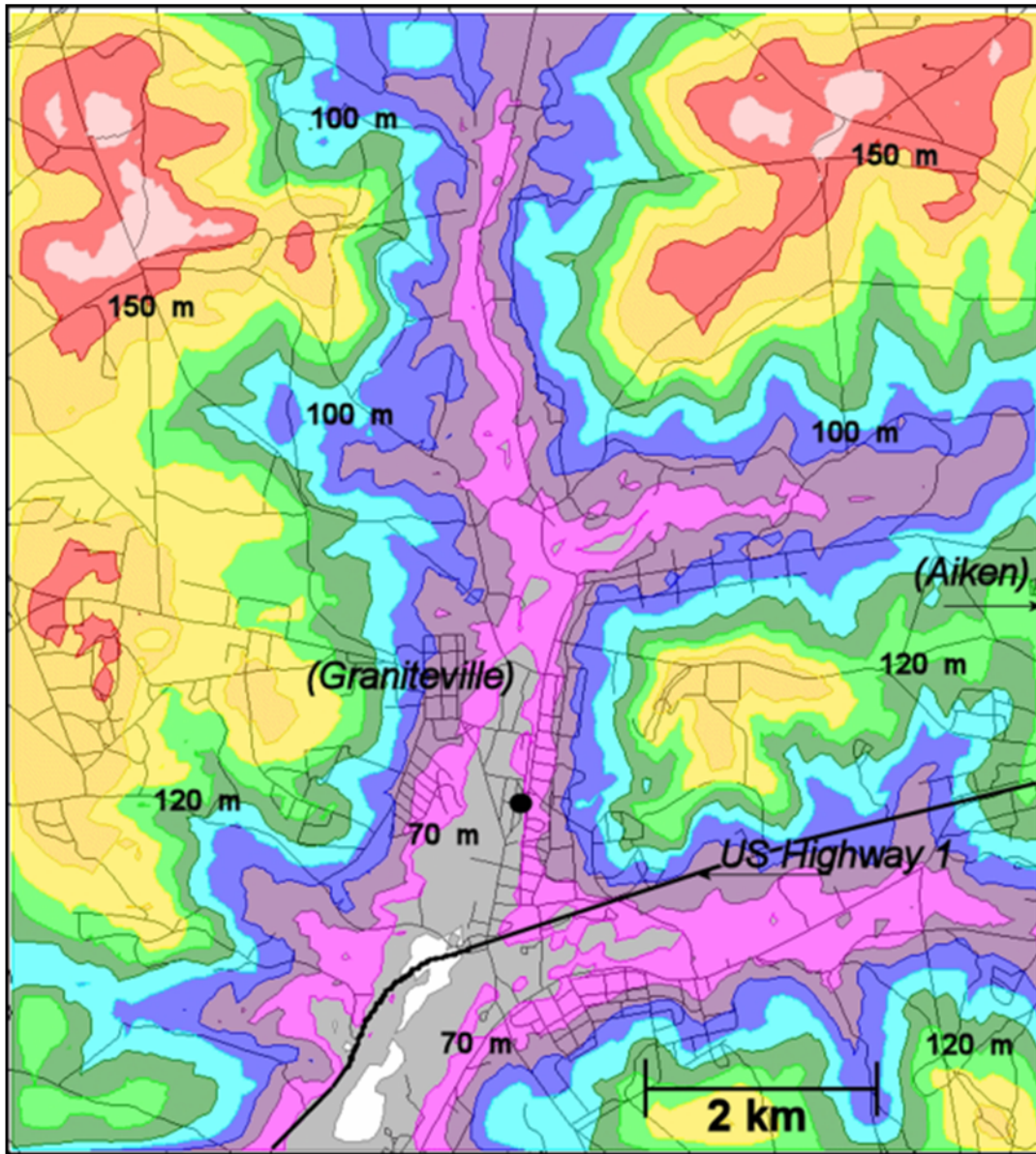


Figure 1: Terrain in the area with contour intervals of 10 meters. Gray and purple shading denotes the lowest elevations, while red and pink shading indicates the highest elevations. Light gray shading indicates topographic elevation exceeding 50 m but less than 60 m AGL while light pink shading indicates topographic elevation exceeding 160 m AGL. The large black circle denotes the derailment site, while lighter lines indicate local roads

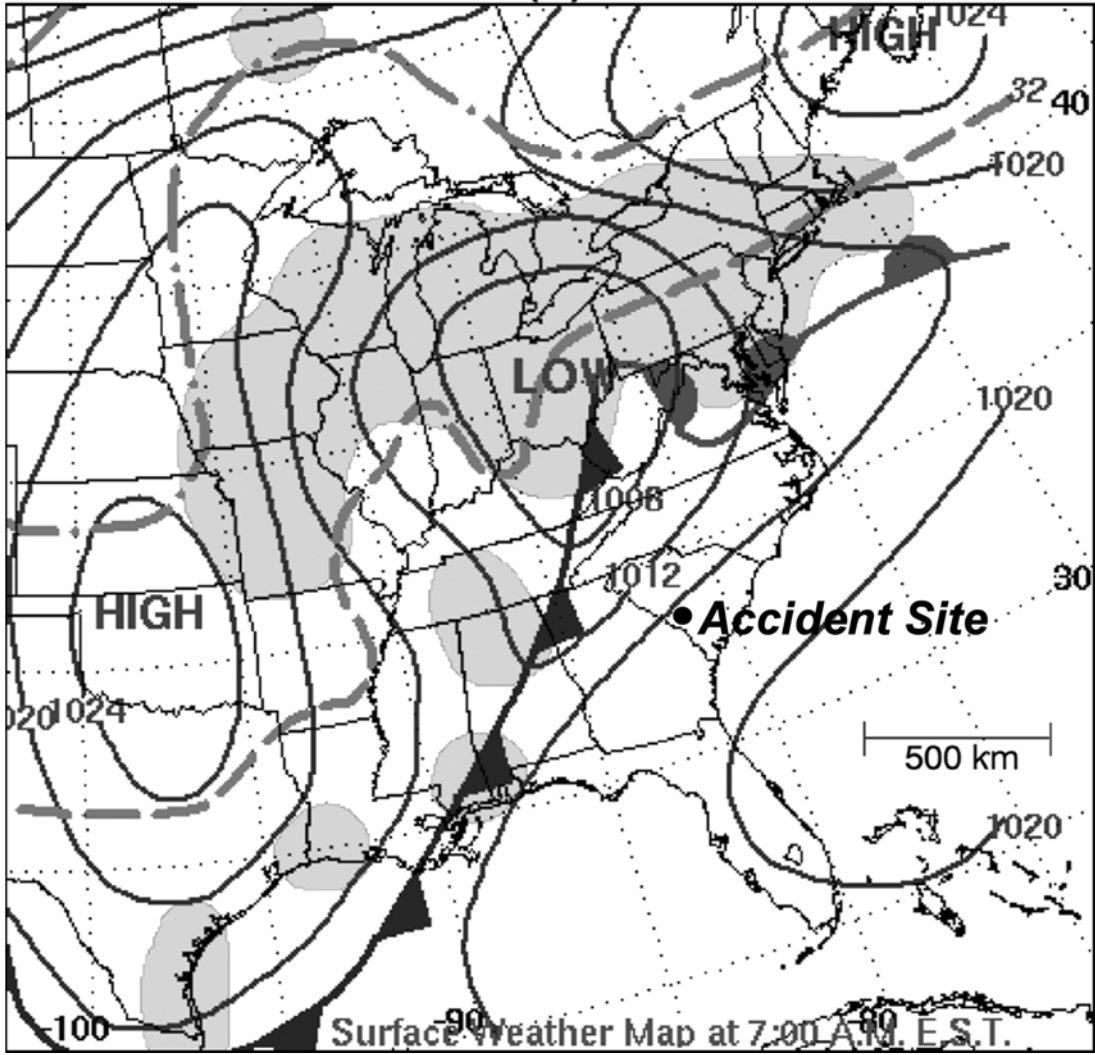


Figure 2: Synoptic conditions at 12 UTC (7:00 a.m. local time) January 6, 2005 (This figure is reproduced from Figure 5 of Buckley et al., 2007).

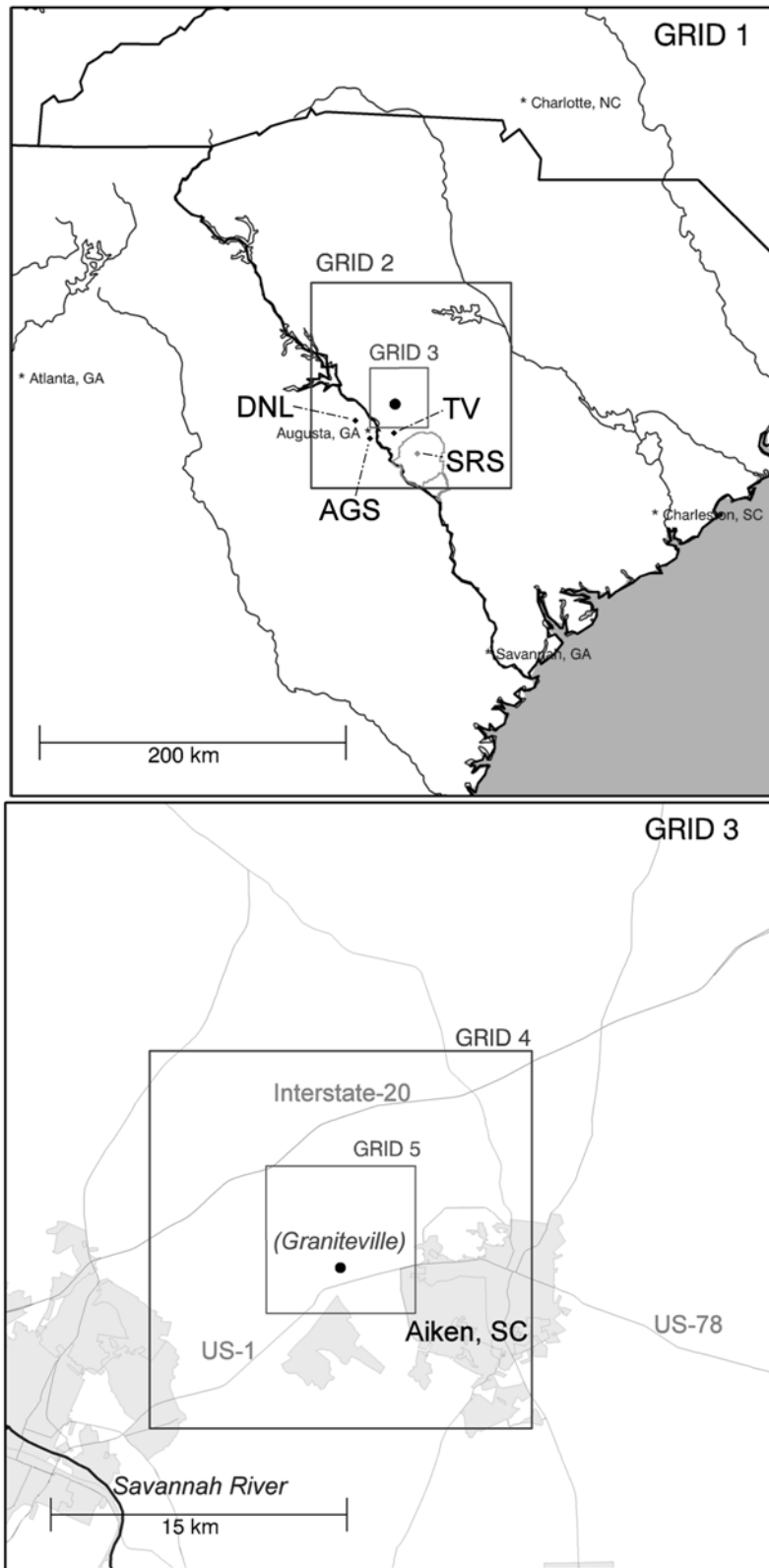


Figure 3: RAMS domains for (a) Outer grids 1, 2, and 3; and (b) Inner grid 4 and 5. The location of nearby meteorological observation towers are indicated with the diamonds labeled “SRS”, “TV”, “AGS”, and “DNL”.



Figure 4: Photograph of the tear in the tank car wall following the train derailment (photo courtesy of SCDHEC (2006)).

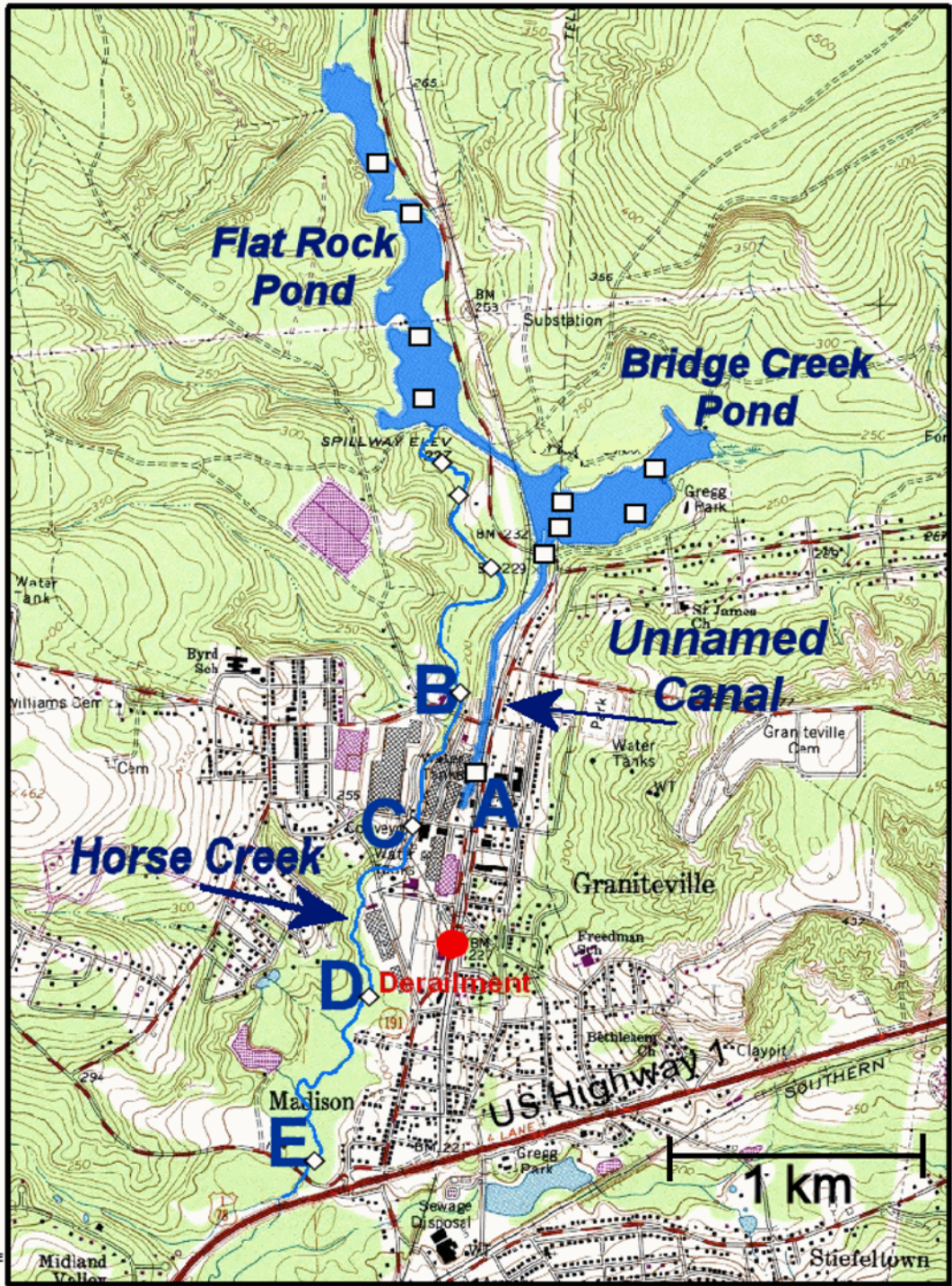


Figure 5: Map of water bodies considered in this study. The derailment site is indicated by the large red circle, while locations used to determine chlorine concentration are indicated by the diamonds (Horse Creek) and squares (lakes and canal). Letter designations are highlighted in Fig. 12.

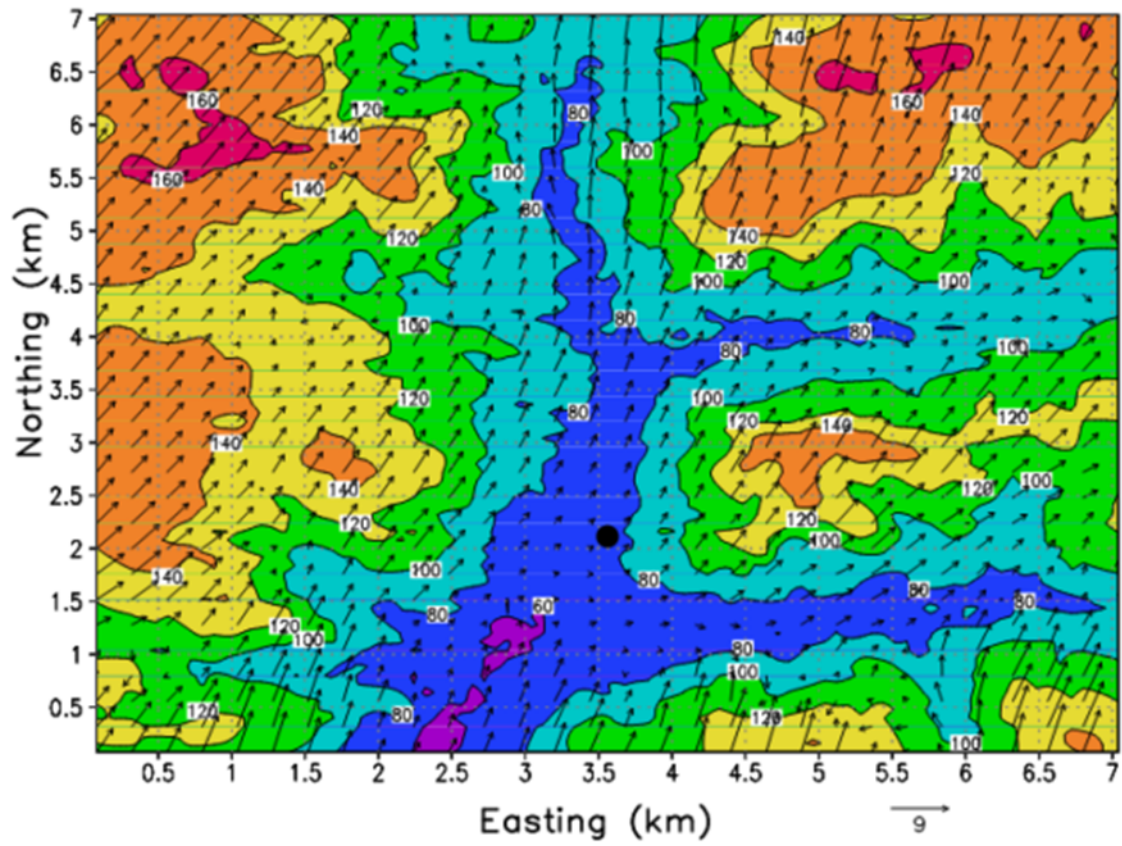


Figure 6: Near surface wind vectors ( $\text{m s}^{-1}$ ) at 0740 UTC, 06 January, 2005. The black circle denotes the derailment site and contour lines indicate topography at 20 m intervals

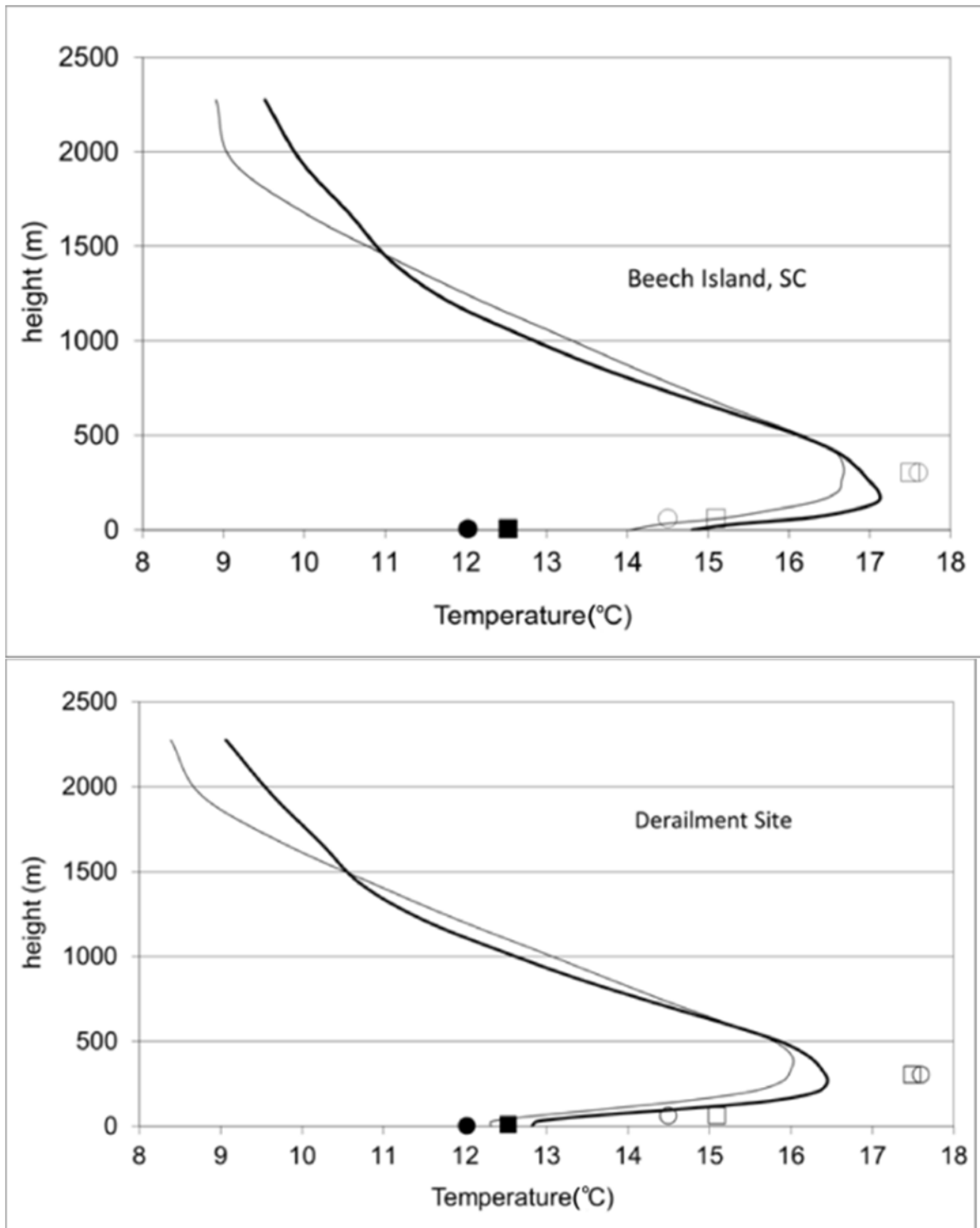


Figure 7: Comparison of simulated soundings for 0740 UTC (thick line) and 0900 UTC (thin line) on 06 January, 2005 at (a) the tall tower site (TV) in Beech Island, South Carolina and (b) the derailment site, with observed data at the climatology site at SRS (filled circle/square at the surface) and at the tall tower (open circle/square at 61 and 300 m). The square markers denote observations at 0740 UTC, while the circles are at 0900 UTC. Locations are noted in Fig. 3a.

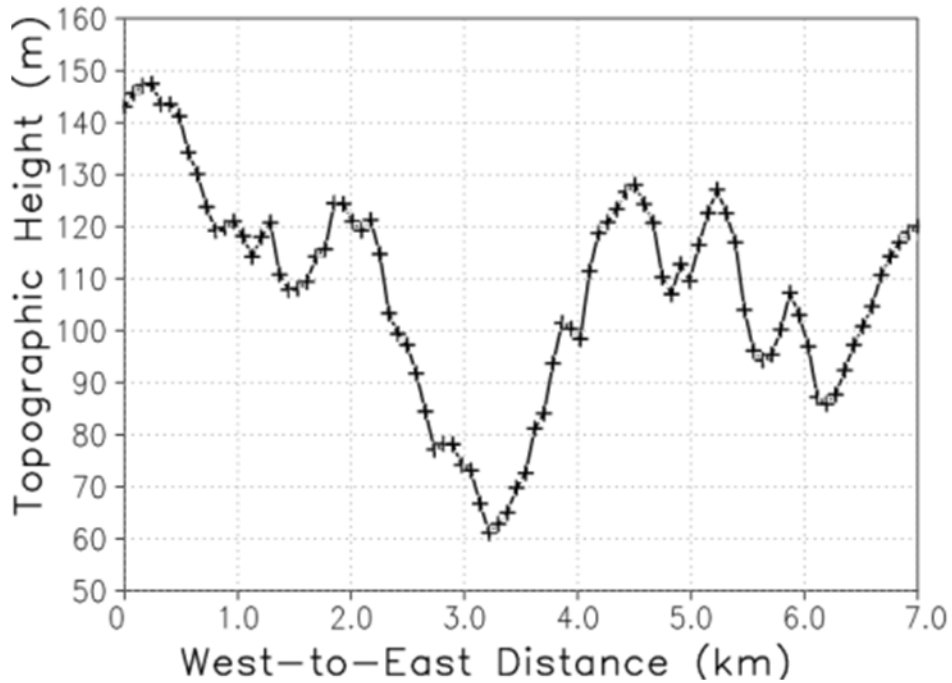
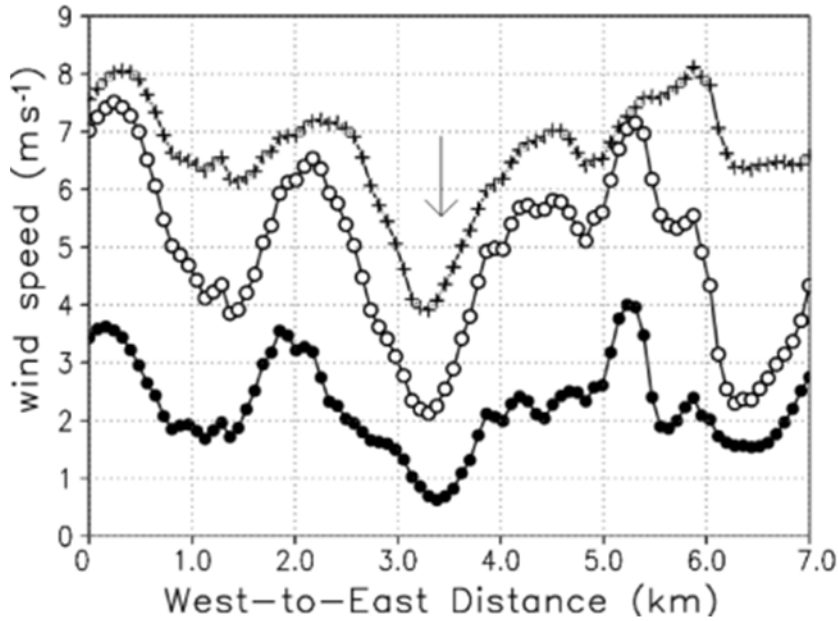


Figure 8: (a) Meridional velocity (i.e., component of the wind blowing due north in  $\text{ms}^{-1}$ ) along an east-west cross-section through the derailment site at 0900 UTC (4:00 a.m. local time), January 6, 2005, at 84 m (crosses), 47 m (open circles), and 15 m (filled circles) above ground level. Axis labeling indicates distance in kilometers, and the arrow denotes the approximate location of the derailment. (b) Topographic height (m) along the same cross-section.

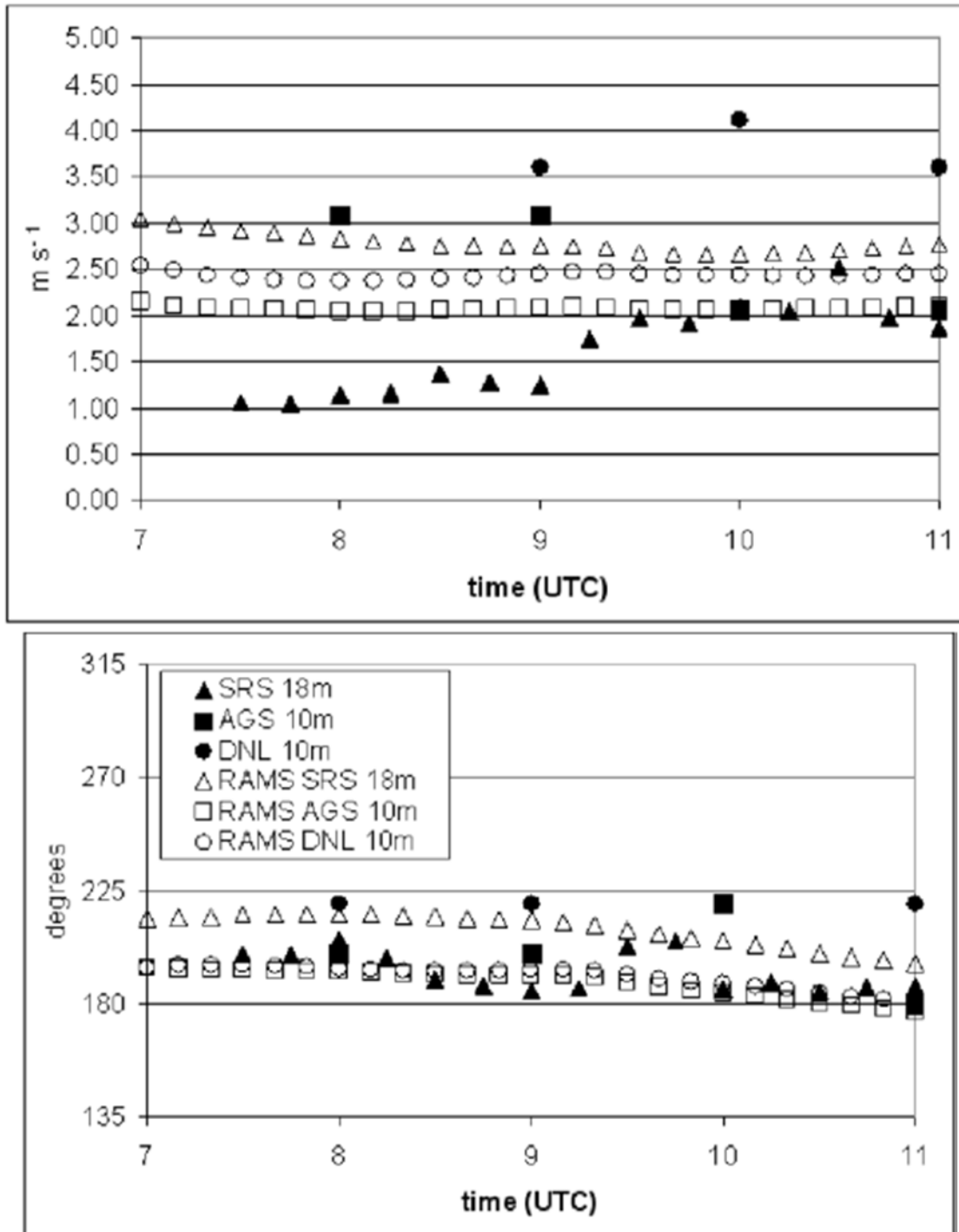


Figure 9: Comparison of simulated and observed (a) windspeed and (b) wind direction between 0700 and 1100 UTC, 06 January, 2005. Model data are interpolated to tower sites on RAMS Grid 2. Locations are noted as “SRS”, “DNL”, and “AGS” in Figure 3a.

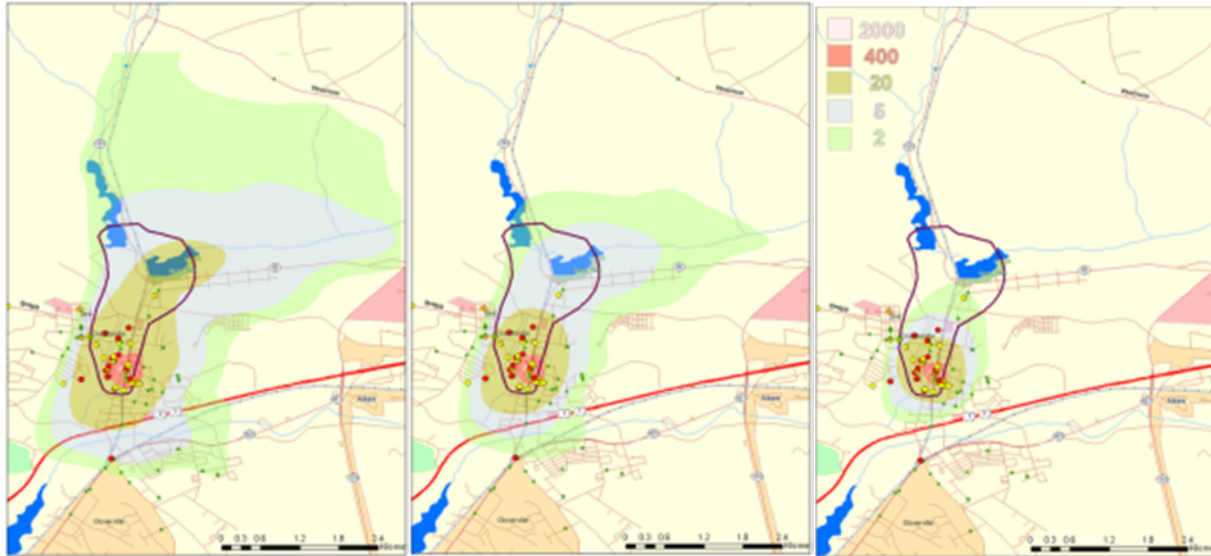


Figure 10: Plots of integrated dose (60-min) for various dry deposition velocities ( $v_d$ ). The dose values (ppm of chlorine) are indicated in the legend. The bold purple line indicates approximate vegetation damage, while the markers denote health effects as discussed in Section 3.2.2. The severity of the cases are ranked by color, where red is the most severe, followed by orange, yellow, green and blue, with blue being the least severe. (a)  $v_d = 0 \text{ cm s}^{-1}$ , (b)  $v_d = 1 \text{ cm s}^{-1}$ , and (c)  $v_d = 3 \text{ cm s}^{-1}$ .

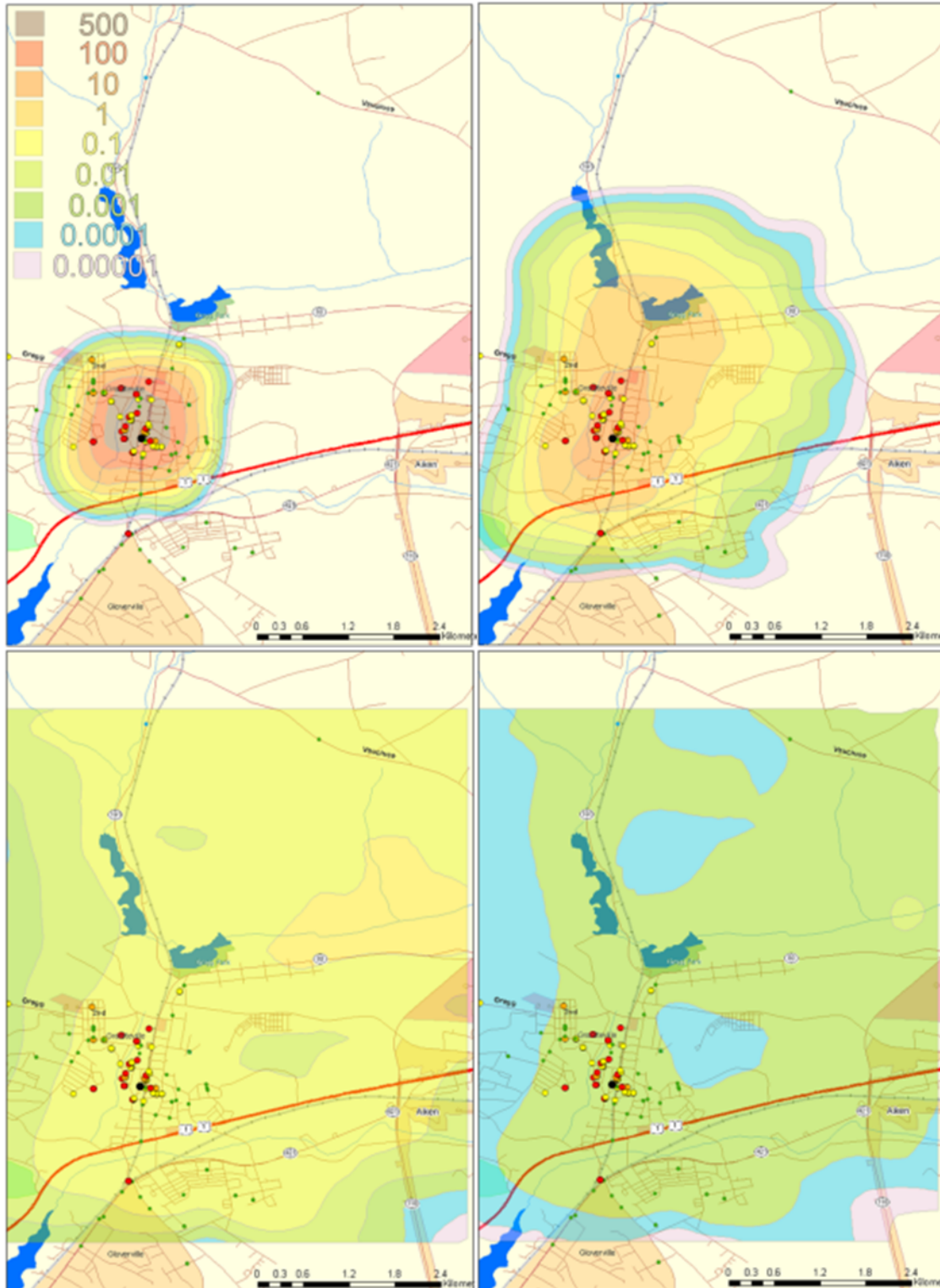


Figure 11: Instantaneous concentration for  $v_d = 1.0 \text{ cm s}^{-1}$  at (a) 10 min, (b) 20 min, (c) 60 min, and (d) 120 min after the start of the release. The ground-level concentration values (ppm of chlorine) are indicated in the legend. The location of the derailment is indicated by the black circle. Markers denote health effects as in Figure 10.

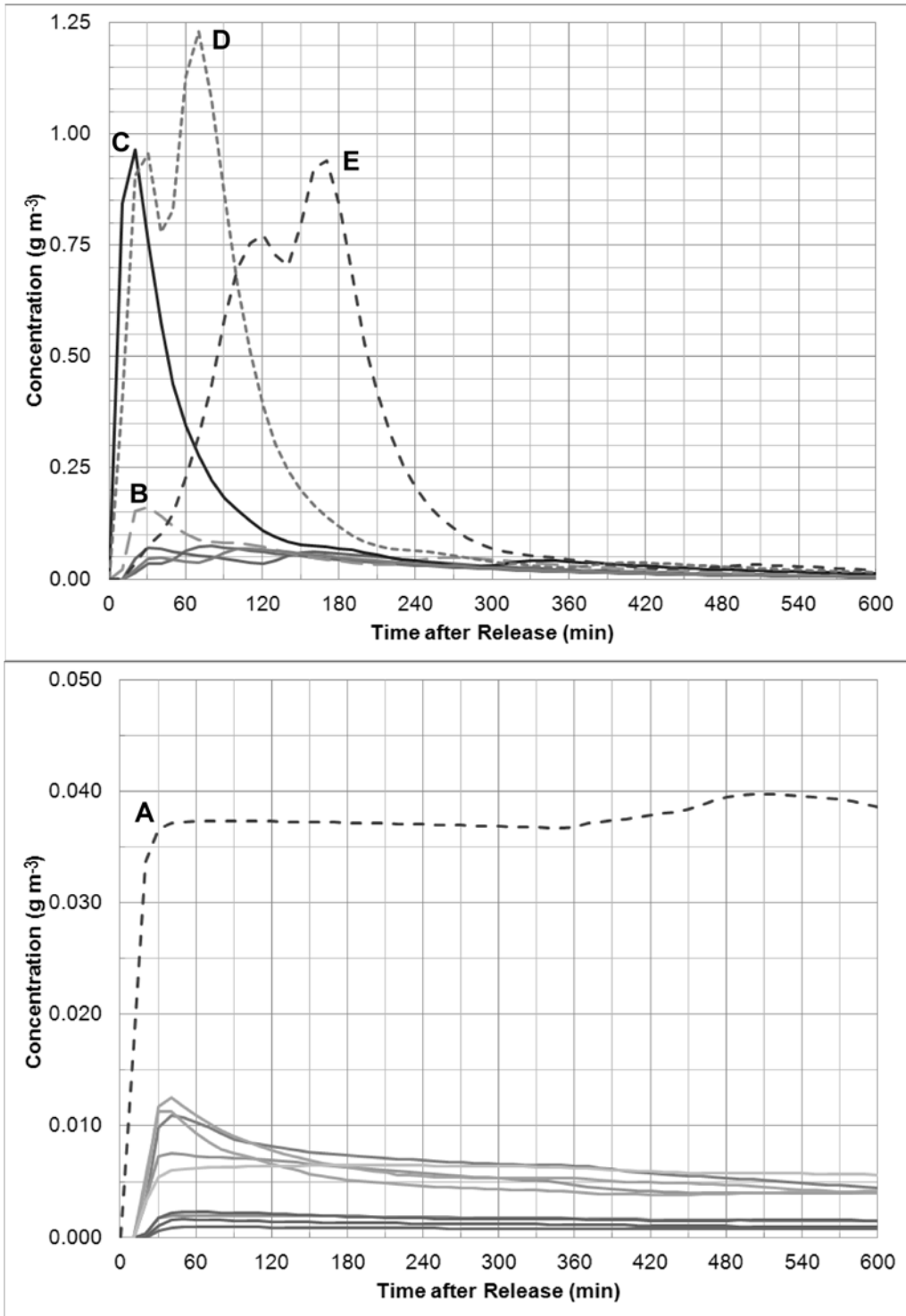


Figure 12: Calculated chlorine concentrations ( $\text{g m}^{-3}$ ) as a function of time at selected location in (a) Horse Creek, and (b) the stagnant water bodies. The locations A to E are indicated in Fig. 5. The unlabeled lines represent much lower concentrations at other marked locations (indicated in Fig. 5 as diamonds along Horse Creek, and squares within the other water bodies).